Geophysical characteristics of the northern Cordillera

N. Hayward[1*] and J.J. Ryan[1]

Hayward, N. and Ryan, J.J., 2021. Geophysical characteristics of the northern Cordillera; in *Northern Cordillera geology: a synthesis of research from the Geo-mapping for Energy and Minerals program, British Columbia and Yukon, (ed.) J.J. Ryan and A. Zagorevski; Geological Survey of Canada, Bulletin 610, p. 145–176. https://doi.org/10.4095/326069*

Abstract: Geophysical data acquired under the Geological Survey of Canada's GEM Cordillera project provide a foundation to a broad range of geological investigations in the northern Canadian Cordillera. For areas of specific geological interest, over 230 000 km of high-resolution aeromagnetic data form a mosaic of comprehensive coverage over a total area of more than 82 000 km^2. The data provide a powerful and valuable legacy data set for current and future activities by the Geological Survey of Canada and academic and industry partners and clients.

Foremost, geophysical data interpretation complements surface geological mapping, especially in inaccessible terrain where bedrock exposure is commonly poor, enabling clearer definition of a region's geology and structure. Beyond applications to bedrock geological mapping, geophysical modelling, integrated with geological results, affords an improved understanding of the deeper crustal structure, leading to new models of the region's tectonic development and mineral deposit context.

Résumé : Les données géophysiques acquises dans le cadre du projet de la Cordillère du programme GEM de la Commission géologique du Canada fournissent les bases sur lesquelles s'appuient un large éventail d'études géologiques menées dans la Cordillère septentrionale au Canada. Dans les régions d'intérêt géologique particulier, plus de 230 000 km de données aéromagnétiques à haute résolution créent une mosaïque procurant une couverture complète sur une superficie totale de plus de 82 000 km^2. Les données constituent un ensemble de données précieux et puissant pour les activités actuelles et futures de la Commission géologique du Canada et de ses partenaires et clients du milieu universitaire et de l'industrie.

Avant tout, l'interprétation des données géophysiques complète la cartographie de la géologie de surface, en particulier dans les terrains inaccessibles où les affleurements du substratum rocheux sont généralement peu nombreux, ce qui permet de définir plus clairement la géologie et la structure d'une région. Au-delà des applications liées à la cartographie géologique du substratum rocheux, la modélisation géophysique, intégrée aux résultats géologiques, permet une meilleure compréhension de la structure plus profonde de la croûte terrestre, ce qui mène à de nouveaux modèles de l'évolution tectonique de la région et du contexte de ses gîtes minéraux.

[1]Geological Survey of Canada, 101-605 Robson Street, Vancouver, British Columbia V6B 5J3
*Corresponding author: N. Hayward (email: nathan.hayward@nrcan-rncan.gc.ca)

INTRODUCTION

Geophysical data acquisition, processing, modelling, and interpretation form a major component of the Geological Survey of Canada's (GSC) GEM Cordillera project. High-resolution (i.e. 400 m line spacing) aeromagnetic data comprise the majority of the geophysical data acquired under GEM Cordillera (Fig. 1). These data directly supported the geological mapping activities and geophysical research, and provide a powerful and valuable legacy data set for future activities by the GSC, provincial and territorial partner agencies, as well as academic, community, and industry clients. Archival geophysical data including GSC regional aeromagnetic (800 m to 1200 m line spacing) and gravity (about 10 km station spacing) data, and LITHOPROBE seismic-reflection and -refraction data, are also important in robust geophysical data analysis, interpretation, and modelling.

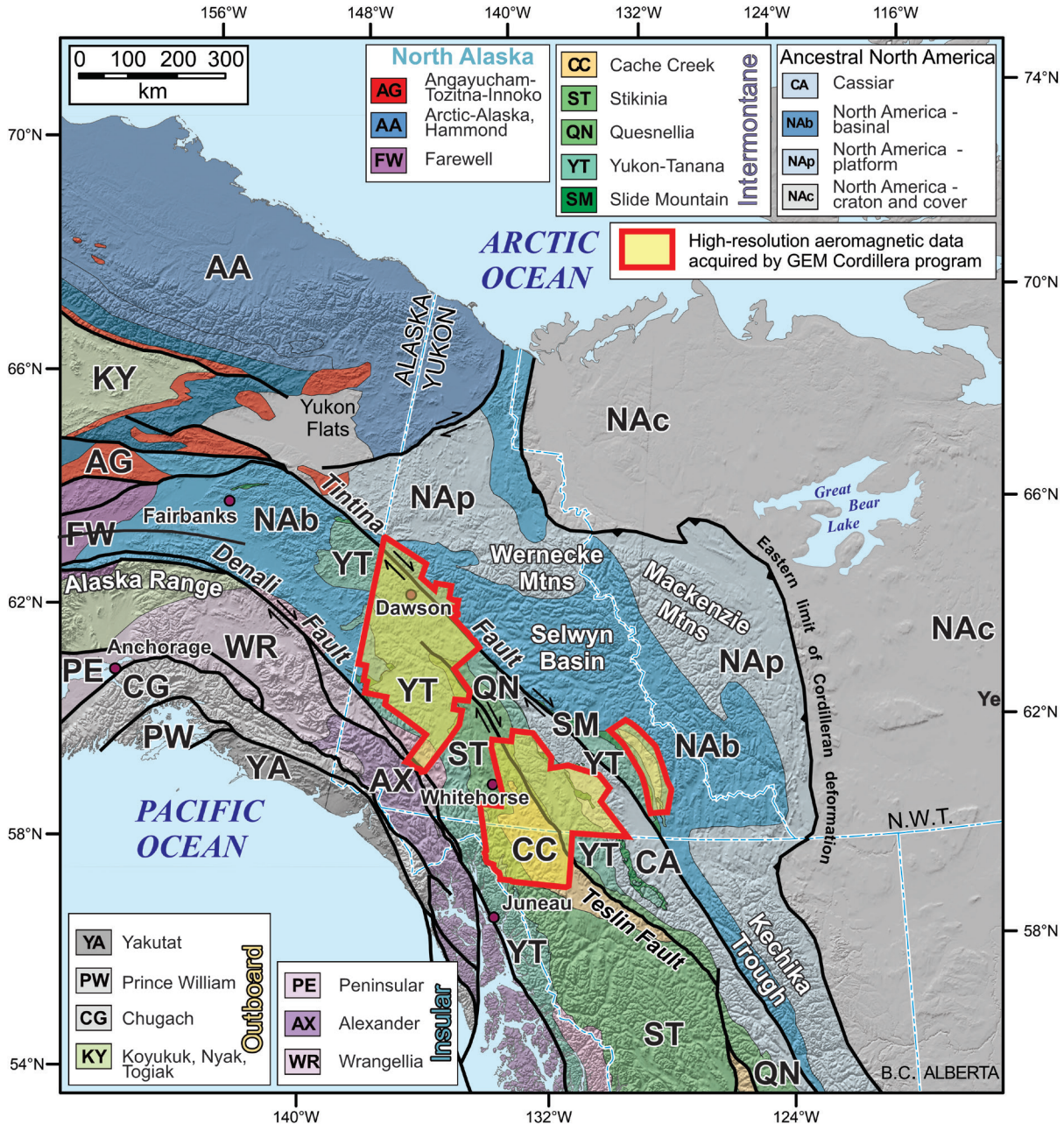

Figure 1. High-resolution aeromagnetic survey coverage acquired under the GEM Cordillera project, shown by areas outlined in red. Major tectonic elements in the Northern Cordillera; *modified from* Colpron and Nelson (2011). Accreted tectonic terranes shown by coloured blocks (*see* legends). The North American craton (NAc), platform (NAp), and basin (NAb) are shown in shades of blue. Heavy black lines show major fault zones.

The geophysical data afford the opportunity to analyze the geology in the third dimension, in order to better understand the geological architecture and history of development of the Cordillera, as well as provide constraints to geological interpretation where physical access is limited.

This paper provides a summary of the geophysical data acquired and the primary geophysical applications, under the GEM Cordillera project between 2008 and 2019. Geophysical applications include the provision of geological and structural interpretations and predictions in support of bedrock geological mapping, regional tectonic interpretations, and detailed studies.

AEROMAGNETIC SURVEYS

Twelve high-resolution (400 m line spacing) aeromagnetic surveys (Carson et al., 2009a, b, c; Kiss and Coyle, 2009a–m, 2011a–g, 2014a–h; Kiss, 2010a–h, 2012a–o; Kiss and Boulanger 2016a–h, 2018a–o; Boulanger and Kiss, 2017a–f, 2018a–h), providing aerial coverage of more than 82 000 km^2, and approximately 234 331 km of line data were acquired under the GEM Cordillera project (Fig. 1 and 2). A summary of the key survey parameters is shown in Table 1. Data were acquired and initially processed and/or levelled by the contractors. Further processing, including calculation

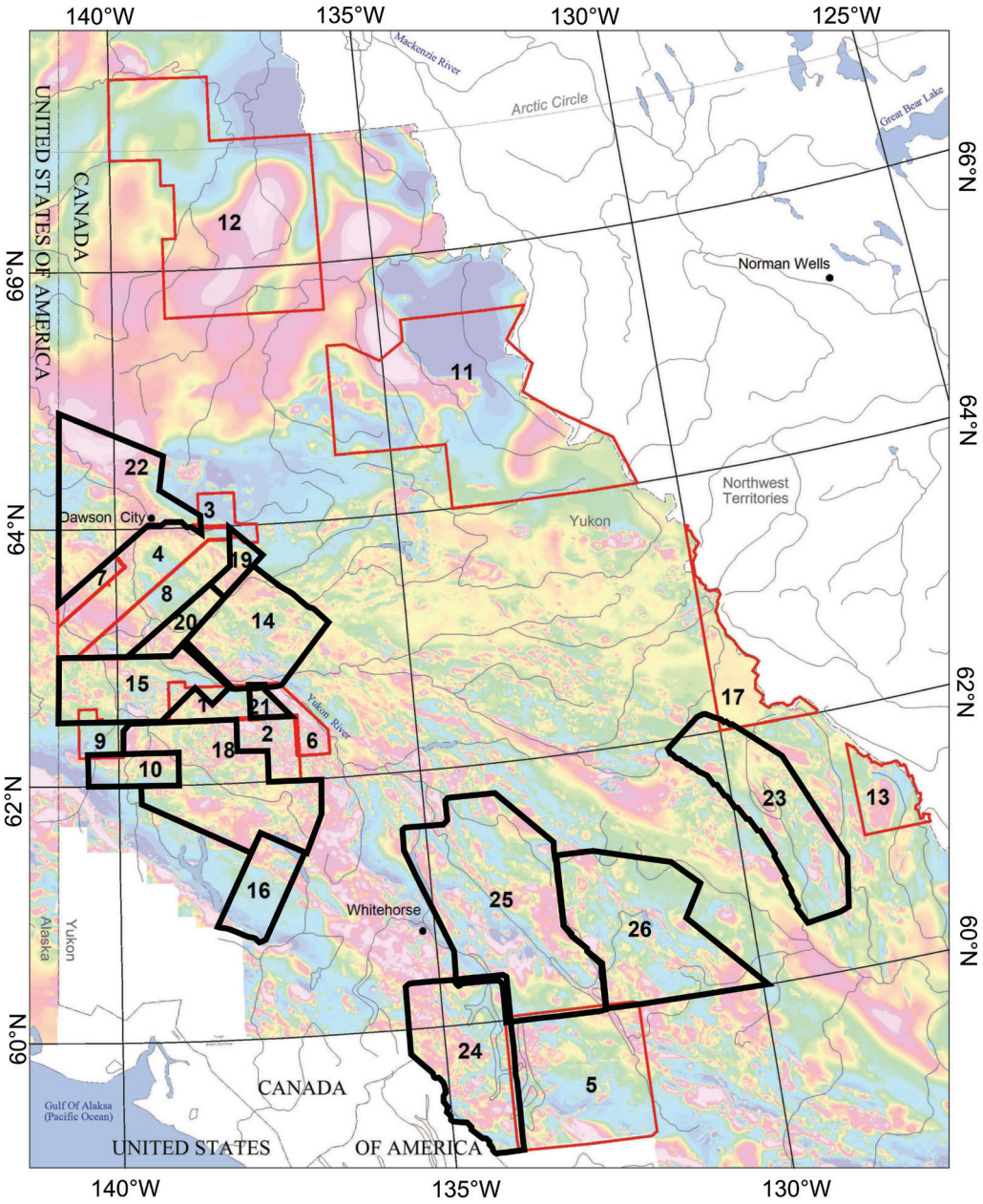

Figure 2. Location of high-resolution aermagnetic surveys acquired under the GEM Cordillera project (heavy black lines; *see* Table1 for index) merged with recent and archival regional aeromagnetic data.

Table 1. Summary of aeromagnetic survey parameters. *See* Figure 2 for locations.

Map index	Survey	Year	Line spacing	Height	Survey type
10	Southern Stevenson Ridge	2008	400 m	125 m	Helicopter
14	McQuesten	2009	400 m	150 m	Fixed wing
15	Northern Stevenson Ridge	2009	400 m	100 m	Fixed wing
16	Kluane	2010	400 m	100 m	Helicopter
18	Nisling River	2011	400 m	100 m	Fixed wing
19	Scroggie Creek Block A	2012	400 m	150 m	Helicopter
20	Scroggie Creek Block B	2012	400 m	150 m	Fixed wing
21	Wolverine Creek	2012	400 m	150 m	Fixed wing
22	Dawson	2014	400 m	150 m	Fixed wing
23	Frances Lake	2016	400 m	120 m	Fixed wing
24	Llewellyn	2017	400 m	150 m	Fixed wing
25	Marsh Lake	2018	400 m	150 m	Fixed wing
26	Wolf Lake	2019	400 m	150 m	Fixed wing

of the residual and first vertical derivatives of the magnetic field, and geophysical compilation was carried out by GSC personnel.

AEROMAGNETIC COMPILATIONS

High-resolution aeromagnetic survey data were compiled iteratively throughout the GEM Cordillera project (e.g. Hayward et al., 2011a, b, 2012) to provide continuous aeromagnetic coverage for regional studies (Fig. 3). Initially survey line data were levelled to a common datum and gridded at a cell size of 100 m, optimal for survey data with a line spacing of 400 m (Table 1).

During the GEM program, a crossborder collaboration was developed between the GSC and the United States Geological Survey (USGS) and the Alaska Division of Geological and Geophysical Surveys (DGGS). This collaboration culminated in the compilation of publically available high-resolution aeromagnetic surveys from Yukon, northern British Columbia, and Alaska, merged with regional aeromagnetic data (Miles et al. 2017; Oneschuk et al., 2019). The compilation (Fig. 4) provides continuous and comprehensive aeromagnetic geophysical coverage of the entire northern Cordillera of Canada and Alaska, large portions of which have poor bedrock exposure.

APPLICATION OF AEROMAGNETIC DATA ANALYSIS TO BEDROCK GEOLOGICAL MAPPING

Aeromagnetic data provide a highly effective complementary data set to geological mapping, especially critical in areas of poor bedrock exposure. Surficial cover, such as vegetation, lakes, soils, and glacial deposits may mask the underlying geology, but be relatively transparent to aeromagnetic signatures that commonly reveal details of the internal character of the geological bedrock units, particularly their structural grain, and the contacts between them. Regional and local structures such as folds and faults may also be delineated.

The best-practice approach employed by the GSC under the GEM Cordillera project was to acquire an aeromagnetic survey prior to a bedrock geological mapping activity. Preliminary interpretation of the aeromagnetic data, with reference to archival geological maps was performed prior to fieldwork. Field geologists carry images of the geophysical data and preliminary interpretations on hand-held personal data assistant devices or electronic tablets, in addition to geological and topographic maps, and satellite imagery, to enable them to directly reference rocks in outcrop to magnetic anomalies. As geologists preplan their geological traverses, they commonly make a route that will test key magnetic anomalies, and attempt to understand their origin

Figure 3. Compilation of high-resolution aeromagnetic data from the Yukon Plateau region, Yukon; **a)** residual total magnetic field, **b)** first vertical derivative (Hayward et al., 2012).

Contents

N. Hayward and J.J. Ryan

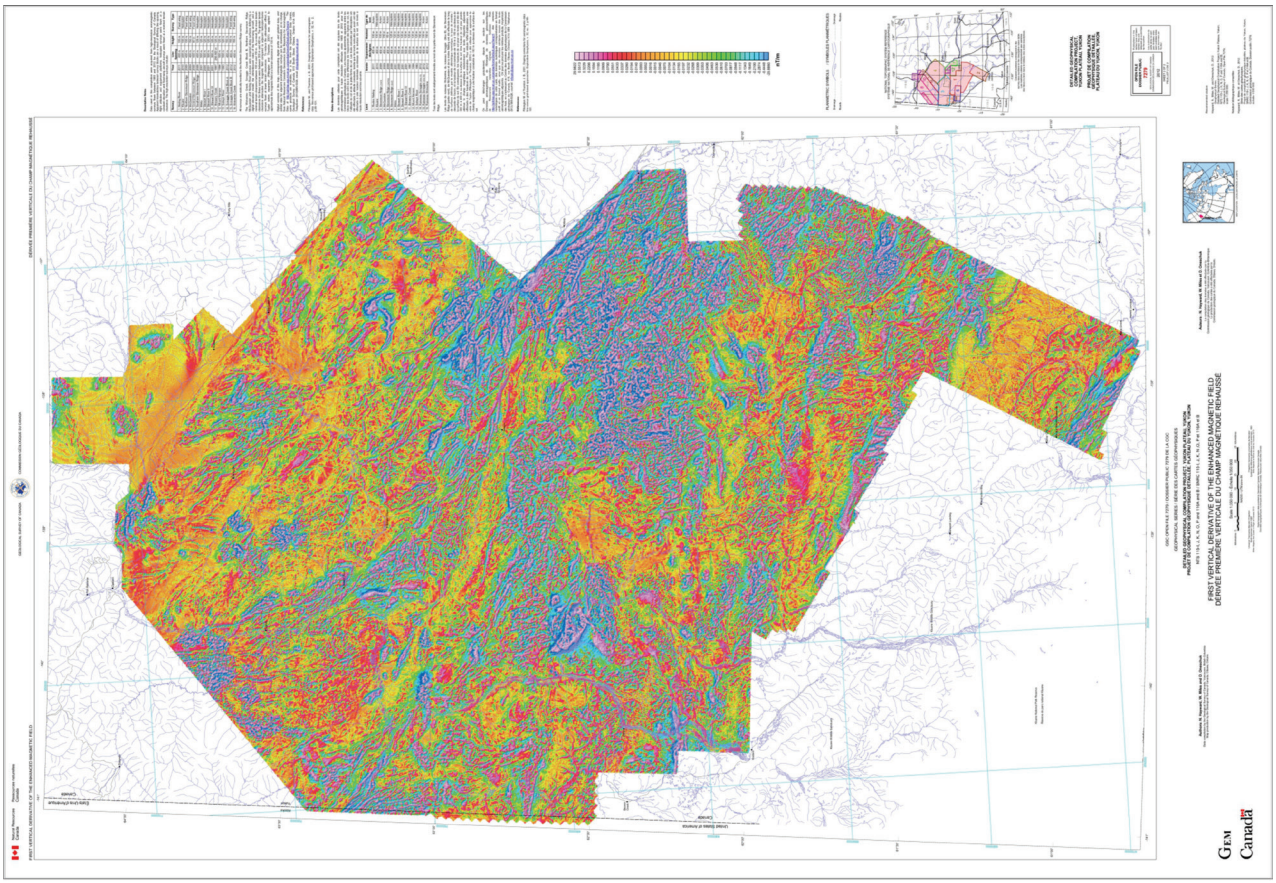

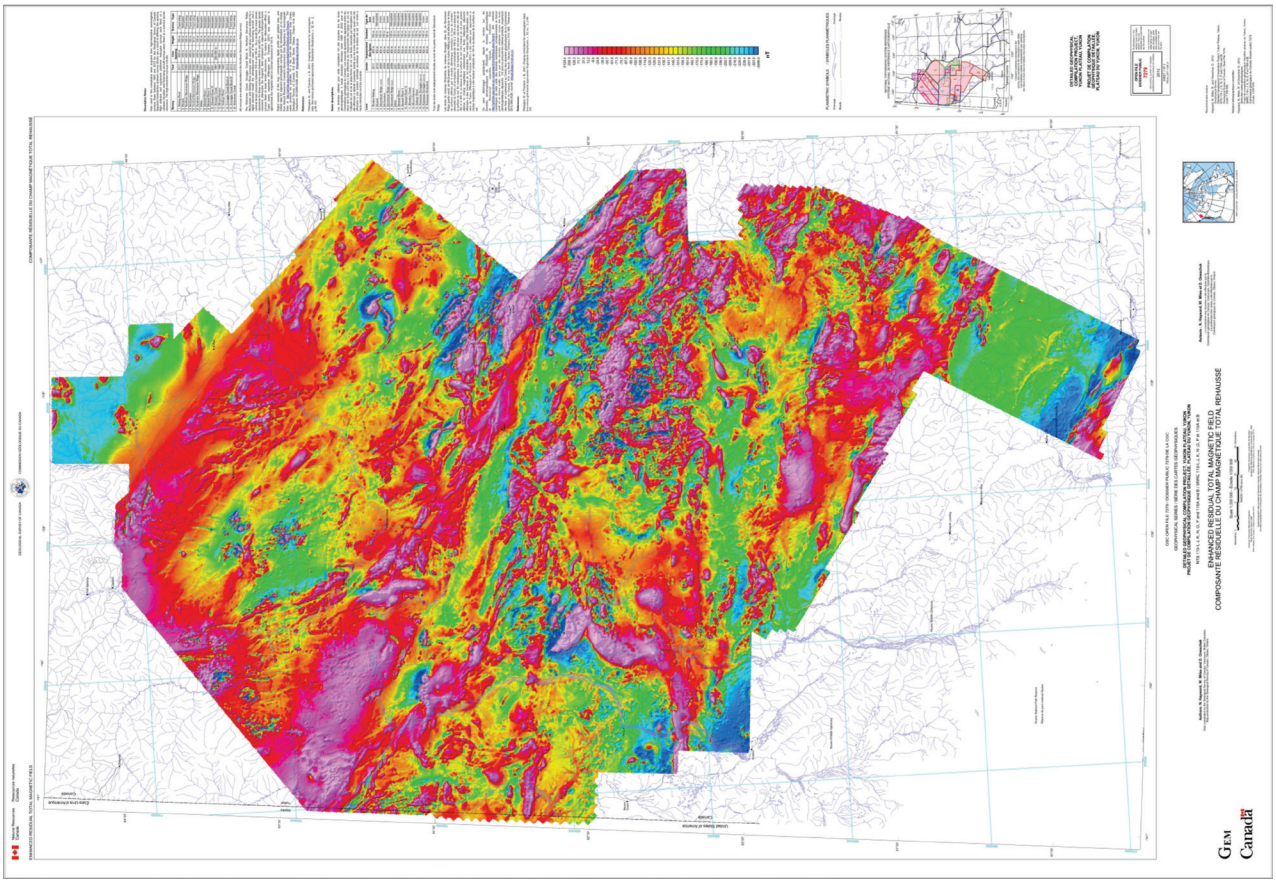

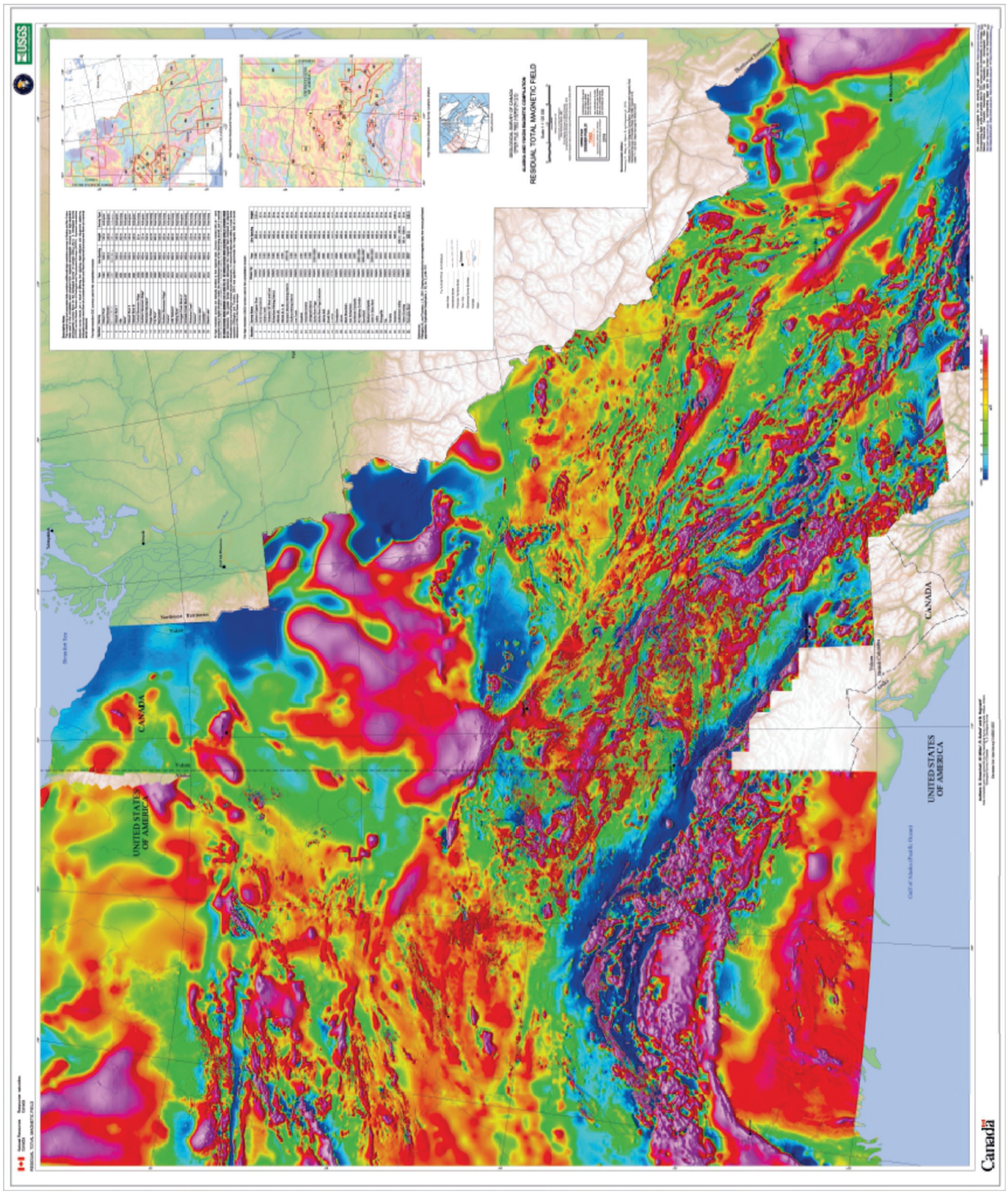

Figure 4. Residual total magnetic field compilation for eastern Alaska, Yukon, and northern British Columbia (Oneschuk et al., 2019).

(e.g. primary mineralogy versus secondary alteration). In addition, field geologists carry hand-held magnetic susceptibility meters (Fig. 5) to enable the recording of direct measurements on the rocks in outcrop to accurately quantify their magnetic properties. These measurements allow on-site interpretation as to whether surface rocks are potential causative bodies for the observed magnetic anomalies. In addition, magnetic susceptibility measurements may be later used as constraints in the building of complex geophysical models in order to investigate a region's three-dimensional geology and structure.

Following bedrock geological mapping, aeromagnetic data are used to constrain and refine geological relationships and structures during production of a regional geological map. The approach of incorporating aeromagnetic data and analysis was applied with great effect throughout bedrock mapping within the GEM Cordillera project. Some examples follow.

Southwestern McQuesten and northern Carmacks map areas, 2009 (parts of NTS 115-I, J, P, and O)

Only preliminary aeromagnetic data were available for southwestern McQuesten and parts of northern Carmacks map areas in advance of fieldwork in summer 2009, and finalized surveys were released later (Kiss and Coyle, 2009a–g); therefore, only a cursory treatment of the data was applied during fieldwork by bedrock mappers. The first author was recruited, and completed aeromagnetic analysis (Fig. 6a) after fieldwork was complete to improve the production of the geological map for southwestern McQuesten and parts of northern Carmacks map areas (Fig. 6b, Ryan et al., 2010). The first vertical derivative of the magnetic field (Fig. 6a) reveals the steepest magnetic gradients, highlighting near-surface features such as faults and geological contacts. Faults and geological contacts may be imaged due to the contrast in magnetic properties between adjacent rock types. In addition, faults may be marked by contrastingly lower or higher magnetic anomalies due to fluid-related alteration along the fault zone. Some of the more striking geological features well highlighted in the aeromagnetic data are the Quaternary volcanic flows of the basalt-dominated Selkirk Group.

Figure 5. Hand-held magnetic susceptibility meter. Photograph by N. Hayward. NRCan photo 2020-596

Northern Stevenson Ridge, 2010 (parts of NTS 115-I, J, K, O)

Aeromagnetic data (Kiss and Coyle, 2009h–m; Fig. 7a) were acquired prior to bedrock geological mapping for the Northern Stevenson Ridge area, carried out mainly in summer 2011. Aeromagnetic data were processed and analyzed in order to interpret the location of faults, geological contacts, and magnetic lineaments (Fig. 7b). During production of the geological maps (Fig. 7d, Ryan et al., 2013a, b), the interpreted magnetic lineations were used to guide the constraint of geological contacts and faults (Fig. 7c) in a region where geological exposure is limited, and a large area covered. Aeromagnetic data provide continuous coverage of many geological features that are not easily observed at the surface, and illustrate the power, and necessity, of aeromagnetic data in support of the production of detailed and accurate geological maps.

Ruby Range, southwest Yukon, 2010 (parts of NTS 115-G, H, A, and B)

The Kluane aeromagnetic survey (Kiss, 2010a–h) was acquired by the Geological Survey of Canada in support of geological field mapping (Israel et al., 2011) by Yukon Geological Survey under the auspices of GEM program colleagues. Processed aeromagnetic data and a detailed interpretation (Fig. 8a), with reference to available geological data were supplied to the YGS mappers prior to bedrock geological mapping and were integral in structural constraint during production of the geological map (Fig. 8b). Geophysical analysis (Fig. 8a) revealed several faults, the contacts between different magmatic phases, and also their internal petrological and/or structural fabric.

Mount Nansen (2015) (parts of NTS 115-H, I, and J) and Klaza River (2016) (parts of NTS 115I and J)

The comprehensive strategy developed during the GEM Cordillera project, of pre-fieldwork aeromagnetic (Kiss and Coyle, 2011a–h) lineament interpretation, crossreference to geophysical interpretations during fieldwork, and the integration of geophysical interpretation with new bedrock

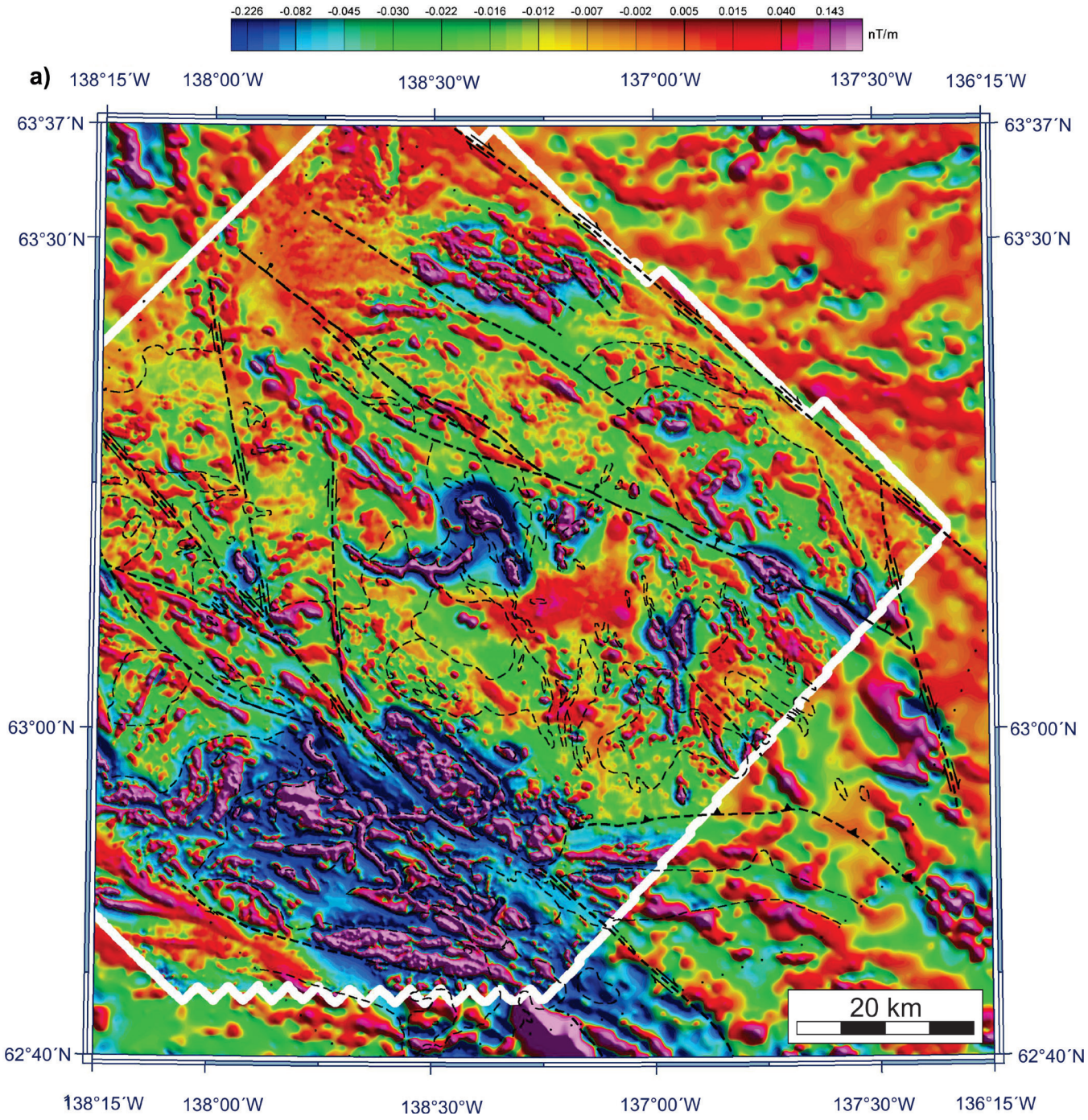

Figure 6. a) First vertical gradient of high-resolution aeromagnetic data. Heavy and light dashed lines show faults and contacts, respectively, interpreted from a combination of aeromagnetic data and geological field observations.

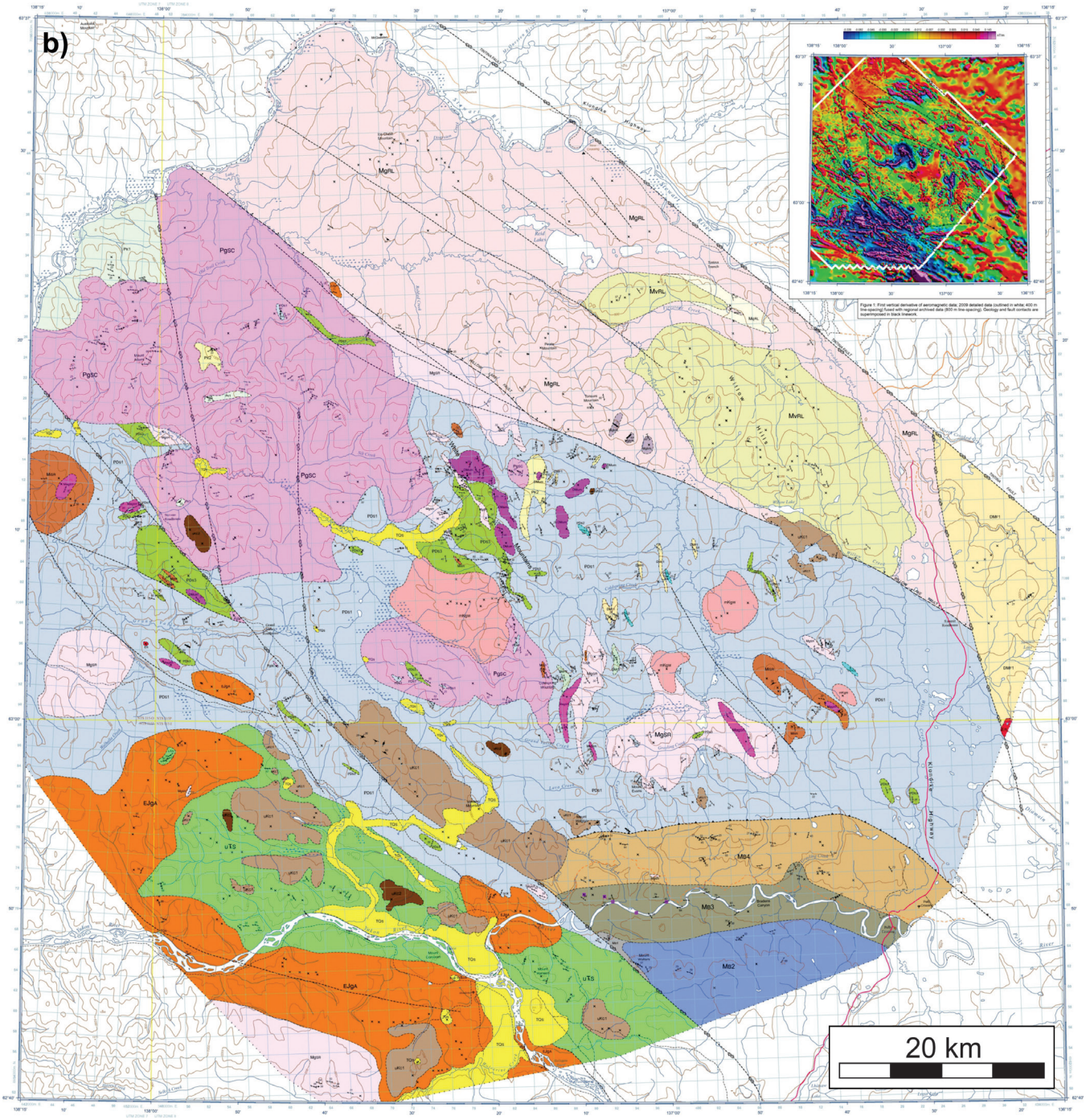

Figure 6. (cont.) b) Final geology map for southwestern McQuesten and parts of northern Carmacks, Yukon (*see* Ryan et al. (2010) for the geological legend).

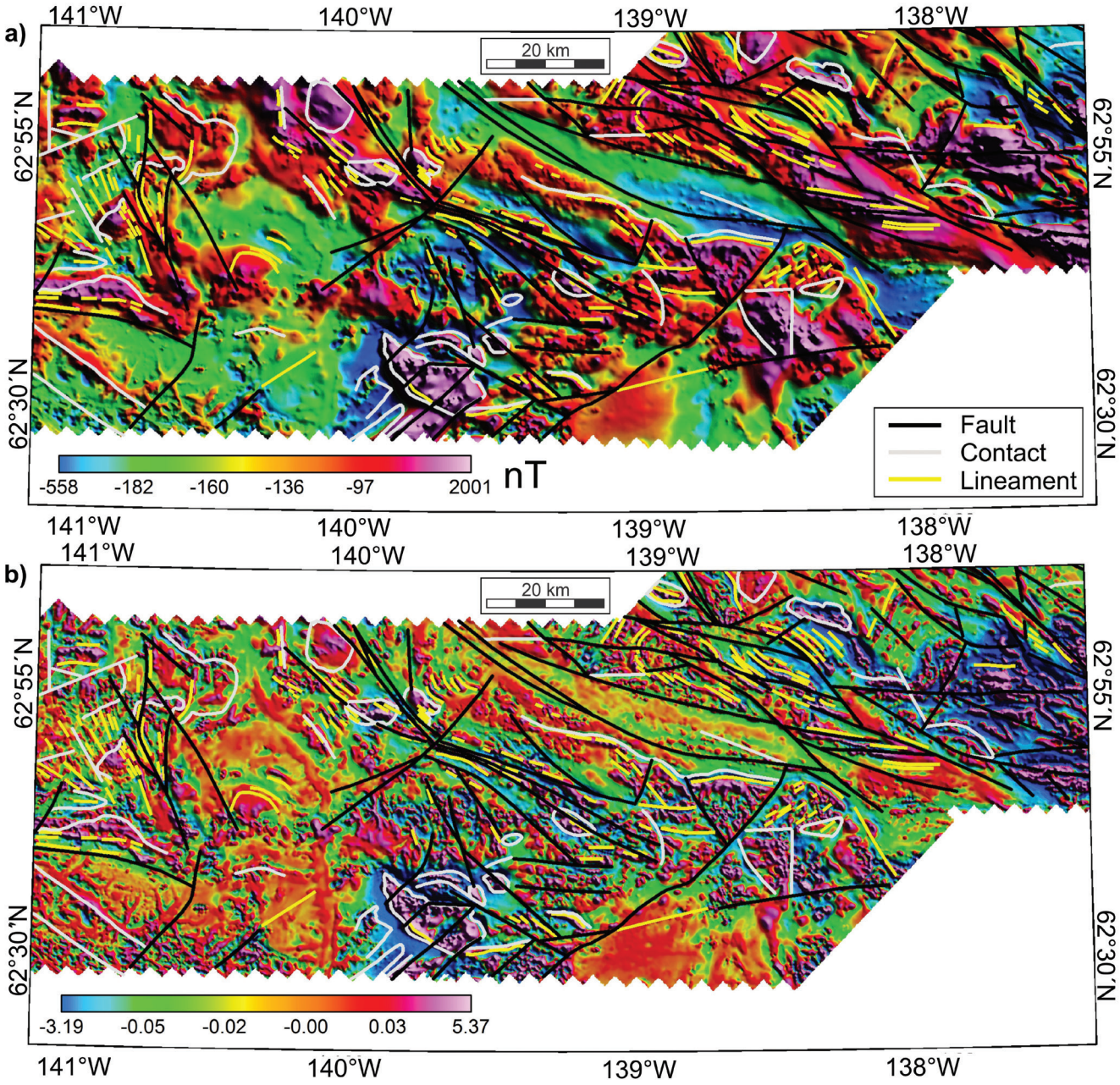

Figure 7. The application of magnetic interpretation in the production of the bedrock geological map for a part of the northern Stevenson Ridge map area (Ryan et al., 2013a, b). **a)** Residual total magnetic field from high-resolution aeromagnetic data. **b)** First vertical gradient of high-resolution aeromagnetic data.

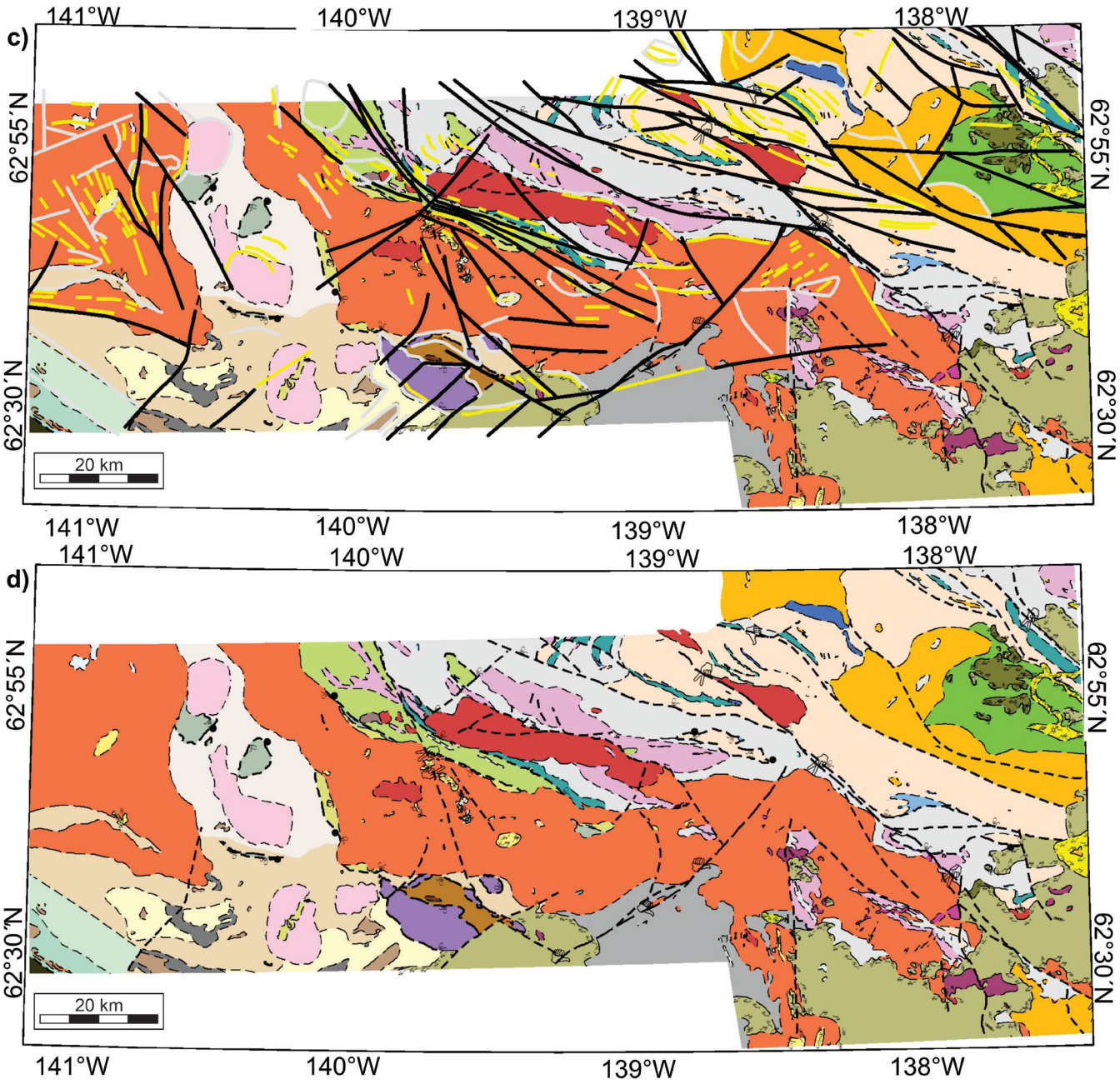

Figure 7. (cont.). The application of magnetic interpretation in the production of the bedrock geological map for a part of the northern Stevenson Ridge map area (Ryan et al., 2013a, b). **c)** Geology with magnetic interpretation. **d)** Final bedrock geology map. Magnetic interpretation: faults = black lines, geological contacts = light grey lines, magnetic lineaments = yellow lines.

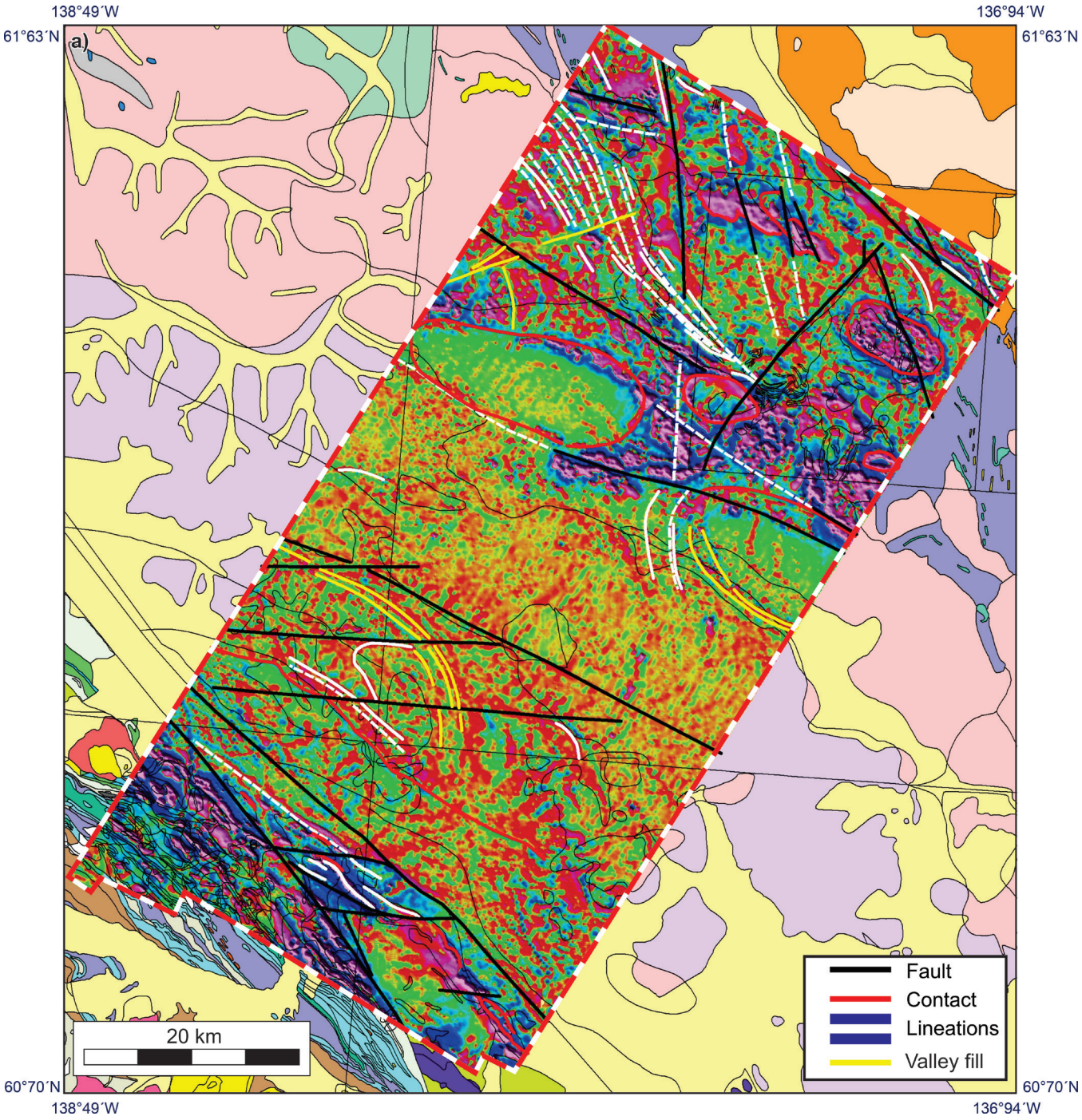

Figure 8. a) Interpretation of first vertical gradient of high-resolution aeromagnetic data (outlined by red-white dashed line) in the Ruby Range area. Black and red lines show faults and contacts respectively. White lines show magnetic lineations. Yellow lines show magnetic features associated with surficial valley fill deposits.

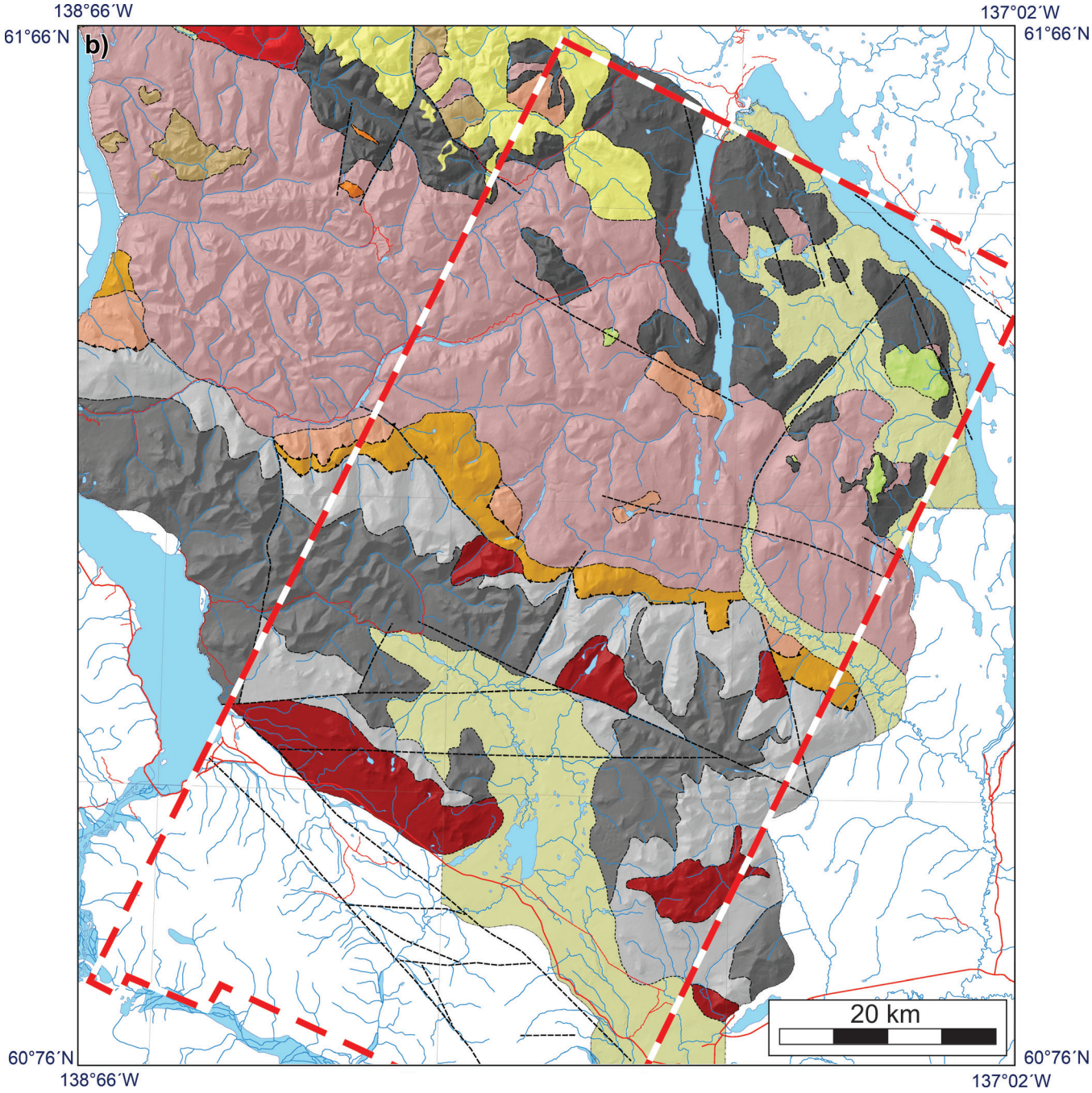

Figure 8. (cont.). b) Geology, Ruby Range, southwest Yukon (*modified from* Israel et al. (2011); *see* legend therein).

geological data during geological map production, was applied to the Mount Nansen (Fig. 9, Ryan et al., 2016) and Klaza River (Fig. 10, Ryan et al., 2018) areas.

Further geophysical surveys and bedrock mapping activities

In 2014 the Dawson aeromagnetic survey (Kiss and Coyle, 2014a–h) was planned in part for evaluation purposes, to elucidate geological features potentially important to mineral exploration that might require additional mapping. Through the referencing of the geophysical results to existing geological maps with spot field checks, it was determined that further mapping was not warranted at this time.

The Frances Lake survey (Kiss and Boulanger, 2016a–h) was flown prior to planned field mapping during 2017. The Geological Survey of Canada was unable to complete the mapping, due to a lack of consent from First Nation communities; however, preliminary fieldwork was completed by the Yukon Geological Survey who released new geological map compilations and interpretations of the area (Moynihan, 2016a, b; 2017), drawing on the preliminary geophysical interpretations.

The Marsh Lake survey (Fig. 2; Boulanger and Kiss, 2018a–h) is being used to support the comparison of the thermochronological history of the region with current structural and tectonic models (Kellett et al., 2017, 2018). Under the Yukon Tectonic evolution activity of the GEM program, rocks have been sampled from across southern Yukon and northern British Columbia, particularly in the Marsh Lake area. Thermochronology is the study of the thermal history of rocks and minerals as they cool either via rock exhumation (erosion and/or tectonic denudation), or changes to the geothermal gradient, or both (e.g. Reiners and Brandon, 2006; Braun 2016). For example, exhumation of the footwall of an extensional fault, cooling of a pluton, relaxation of the geothermal gradient following orogenesis, volcanic eruption of magma, or erosion of elevated topography in mountainous regions may all cause rocks and minerals to experience progressively lower temperature conditions from some initial thermal condition. Since there are a range of geological processes that can lead to rock cooling, the authors' ability to link thermochronological ages to geological history depends on how well the geological setting of the samples is understood. The new Marsh Lake aeromagnetic survey therefore allows identification of potential buried plutons that could have influenced the thermal history of the samples. The authors are testing a number of hypotheses in the Marsh Lake area about the structural and tectonic history of the Intermontane terranes (particularly, the timing and kinematics of the Crag Lake, Teslin, and Nahlin faults, and Mesozoic sedimentary basin evolution). Ability to test these hypotheses using thermochronological data hinges on the new Marsh Lake aeromagnetic survey.

The Wolf Lake survey (Fig. 2; Kiss, 2019a–l) covers both the Thirtymile Range and Wolf Lake regions, where geological mapping was performed in 2018 (Cleven et al., 2018). The study area is situated to encompass rocks that may span a suture zone that involved a major orogenic event related to the accretion of the Yukon-Tanana terrane to the North American margin (van Staal et al., 2018). The region exhibits a high range of magnetic amplitudes. This may result from a high contrast in the magnetic properties of the geological units such as the variation from highly magnetic serpentinized peridotite to interstratified metasedimentary units, but the region also exhibits many magnetic lows due to a concentration of fault and shear structures. The new high-resolution aeromagnetic survey will be used to help trace and delineate both units and structures through regions with extensive overburden. It will also aid in understanding the large-scale structural patterns, since ductile deformation such as folding and shearing are visibly interpretable from the imagery. These interpretations will be synthesized with outcrop data, observations, and analytical results to create and refine a tectonic model for the region.

APPLICATION OF POTENTIAL FIELD DATA TO INVESTIGATIONS INTO THE CRUSTAL STRUCTURE AND TECTONIC DEVELOPMENT OF THE CORDILLERA

The tectonic history of the Cordillera was investigated through the analysis aeromagnetic and geological data newly acquired within the GEM Cordillera project, integrated with archival geological and geophysical data (e.g. Yukon Geological Survey, 2018; Geological Survey of Canada, 2019a, b).

Crustal lineaments and their control on structure and mineralization

Hayward (2015) restored regional aeromagnetic, gravity (Fig. 11a), and topographic data (Fig. 11b) for about 430 km of post-Cretaceous dextral displacement on the Tintina Fault. A northwest-trending lineament, the Liard line, is interpreted from the geophysical data to be related to

Figure 9. a) Residual total magnetic field from high-resolution aeromagnetic data. Heavy and light dashed lines show faults and contacts respectively, interpreted from a combination of aeromagnetic data and geological field observations. Young northwest-striking faults form prominent features in the east side of the data. **b)** Final geology map of the Mt. Nansen area, Yukon (Ryan et al., 2016)

Contents

N. Hayward and J.J. Ryan

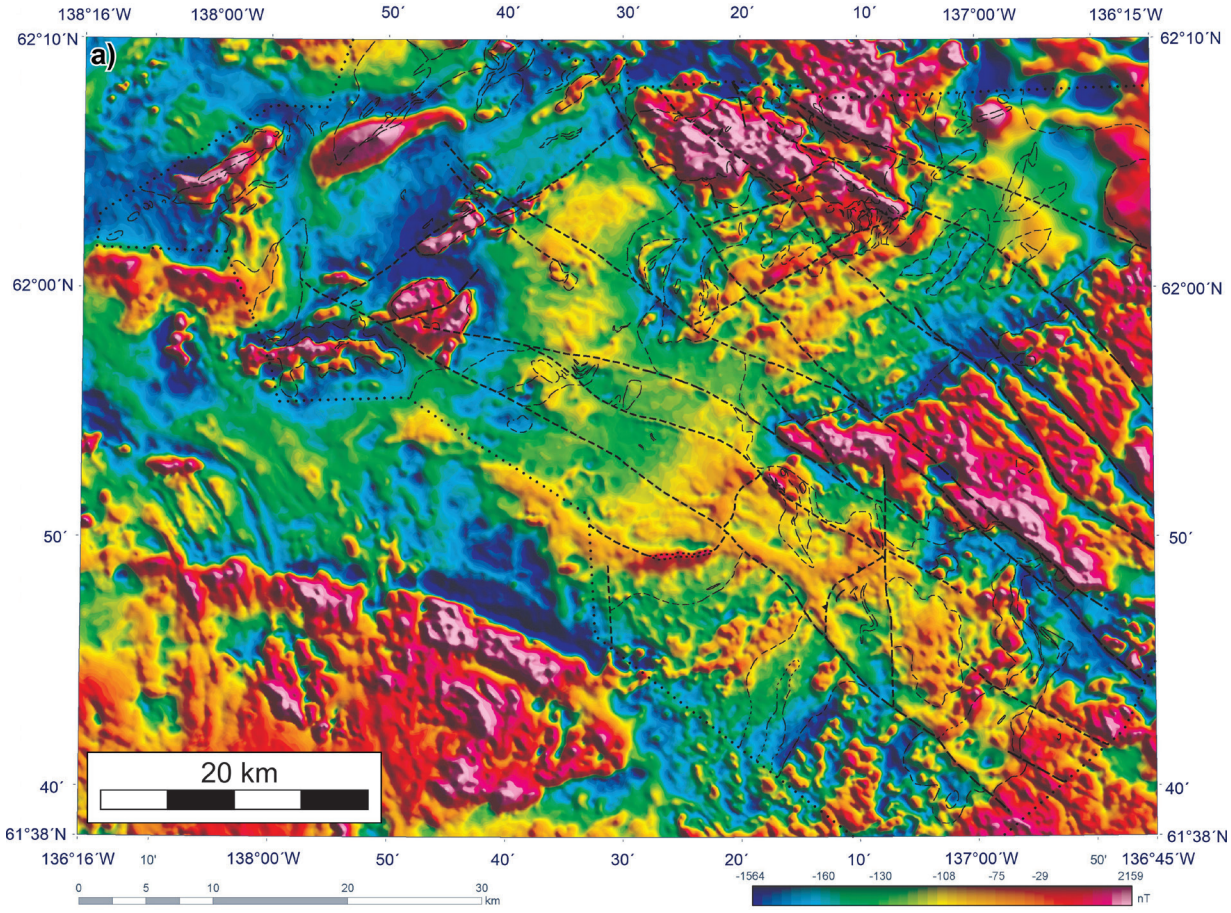

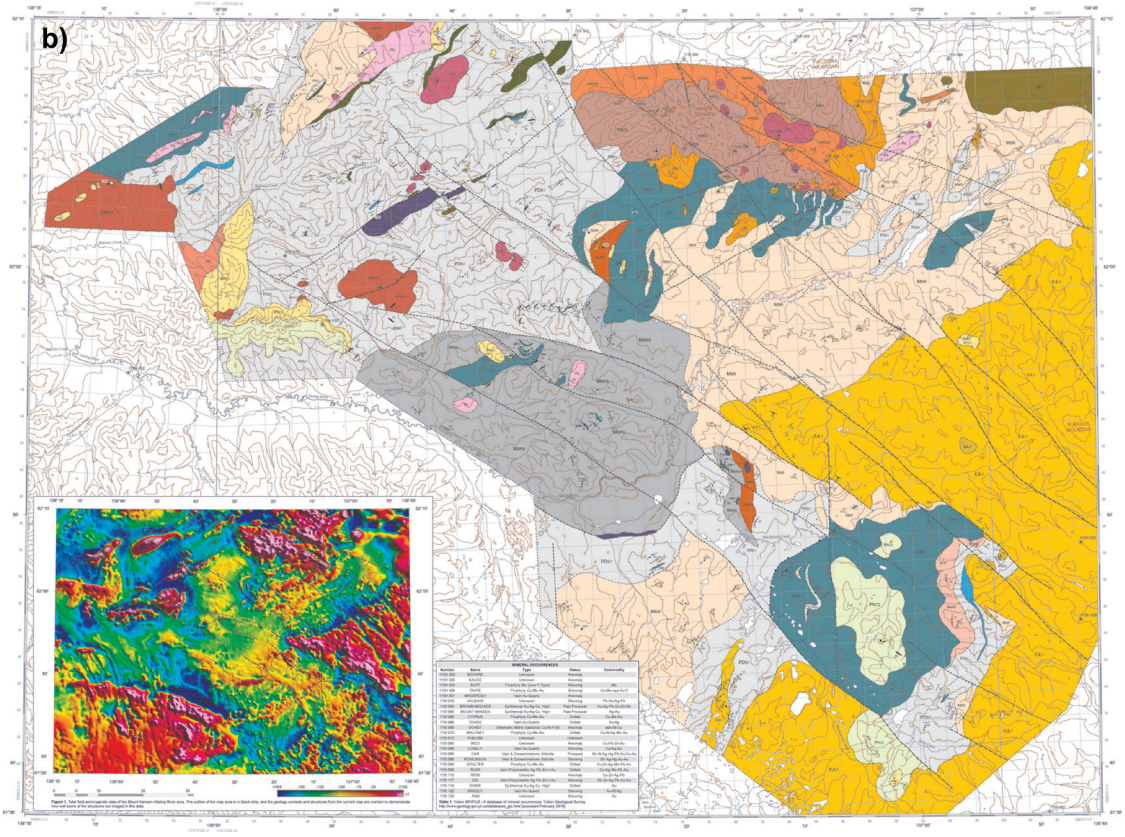

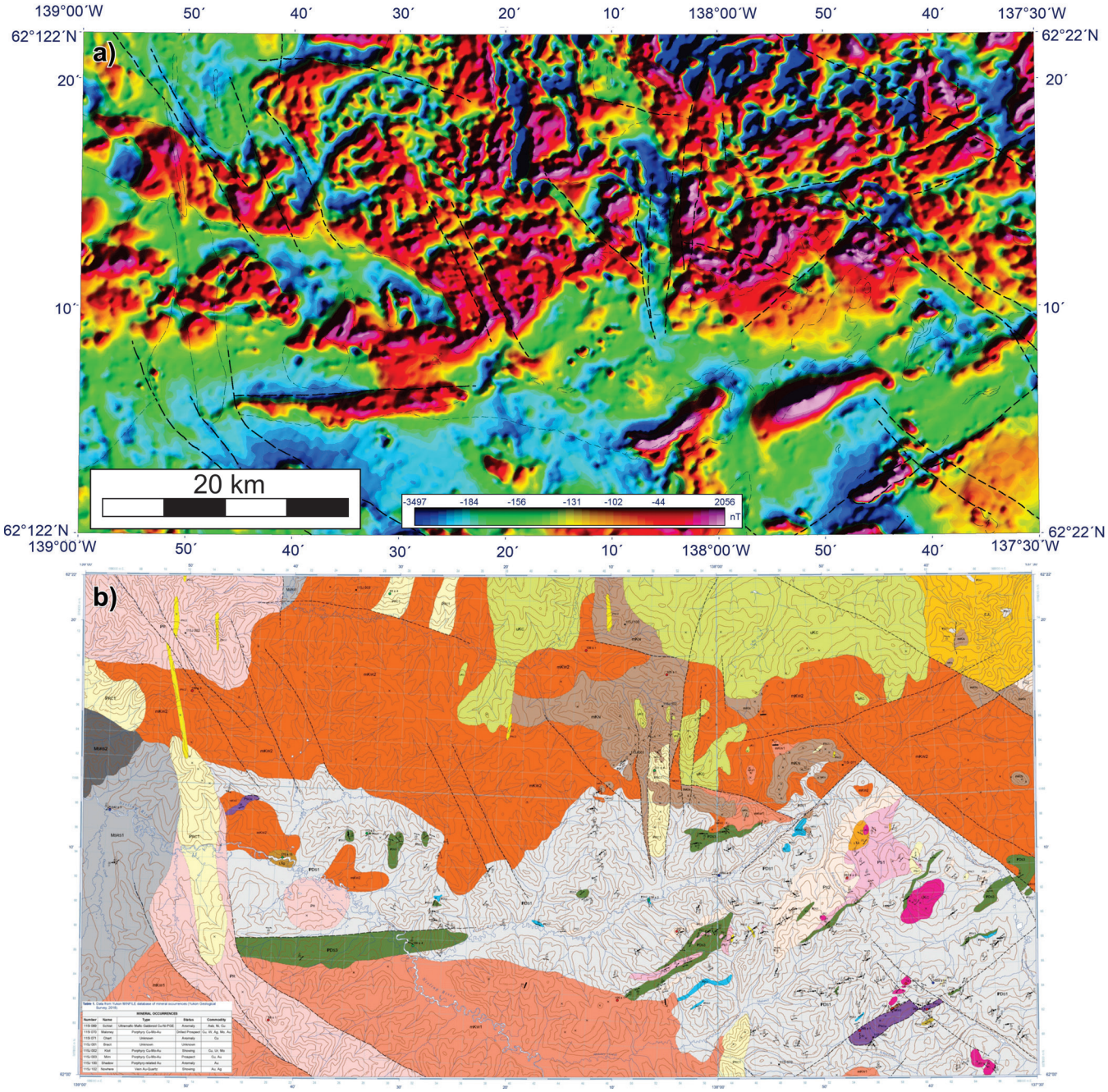

Figure 10. a) Residual total magnetic field from high-resolution aeromagnetic data. Heavy and light dashed lines show faults and contacts respectively, interpreted from a combination of aeromagnetic data and geological field observations. **b)** Final geology map of the Klaza area (Ryan et al., 2018).

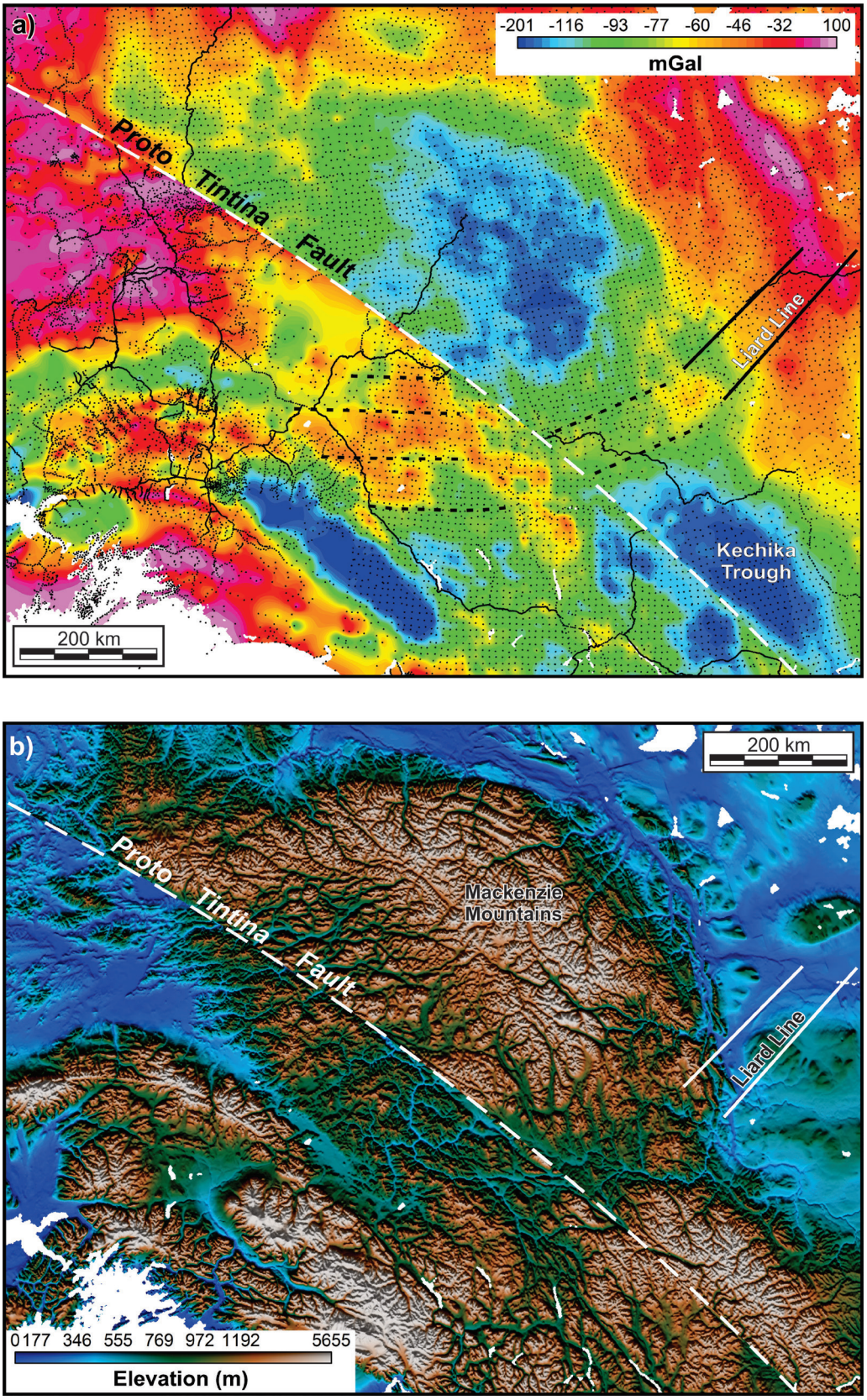

Figure 11. Restoration of **a)** Bouguer gravity anomaly and **b)** topography for about 430 km of right-lateral strike-slip displacement along the Tintina Fault (Hayward, 2015).

structures within the lower crust and/or mantle lithosphere. Three-dimensional density models derived from the inversion of Bouguer gravity data reflect a regional change in the density of the crust associated with the lineament. The lateral extent of the structure suggests the continuity of North American basement rocks as far west as the Denali Fault.

The recognition of lithospheric lineaments, from their manifestation in geophysical, geological, and topographic data, suggests that they may have influenced Mesozoic mineralization through influence on the development of the shallow crustal structure, intrusion, and exhumation and erosion (Fig. 12); *see* Hayward (2015) for discussion.

A regional scale décollement in the Cordillera of northern Canada and Alaska

Hayward (2019) presented the results of a new approach to the 3-D inversion and interpretation of gravity data, applied to the investigation of the crustal structure of the northern Cordillera of Canada and Alaska. A popular science article (Cook, 2019) in the American Geophysical Union journal EOS (Earth and Space Science News) also highlighted the results. The 3-D density model, derived from the 3-D gravity inversion, defines the distribution, geometry, and depth extent of low-density rocks, interpreted to be primarily related to mid-Late Cretaceous granitic intrusions (Fig. 13). The regional variation in the depth extent of the low-density rocks is interpreted to be associated with a regional décollement, a system of large shallow-dipping detachments and faults that shallows toward the northeast from a depth of about 15–20 km beneath Selwyn Basin to about 11 km beneath the Mackenzie Mountains (Fig. 14). The décollement is interpreted as syntectonic with, or postdating, the intrusions, but predating and displaced about 430 km by the Eocene Tintina Fault. Through comparisons with the trend of surface faults, and geological cross-sections, the décollement is inferred to be related to the middle Cretaceous and Paleocene formation of the Mackenzie Mountains fold and thrust belt, with a 035° direction of shortening.

Structural aspects of the Intermontane terranes

The tectonic history and structure of the northern Intermontane terranes and associated sedimentary basins (Fig. 15) were investigated by Calvert et al. (2017). An elongate, Mesozoic sedimentary basin that extends over 650 km from northern British Columbia to the region of Carmacks, Yukon has an underexplored mineral potential due to limited

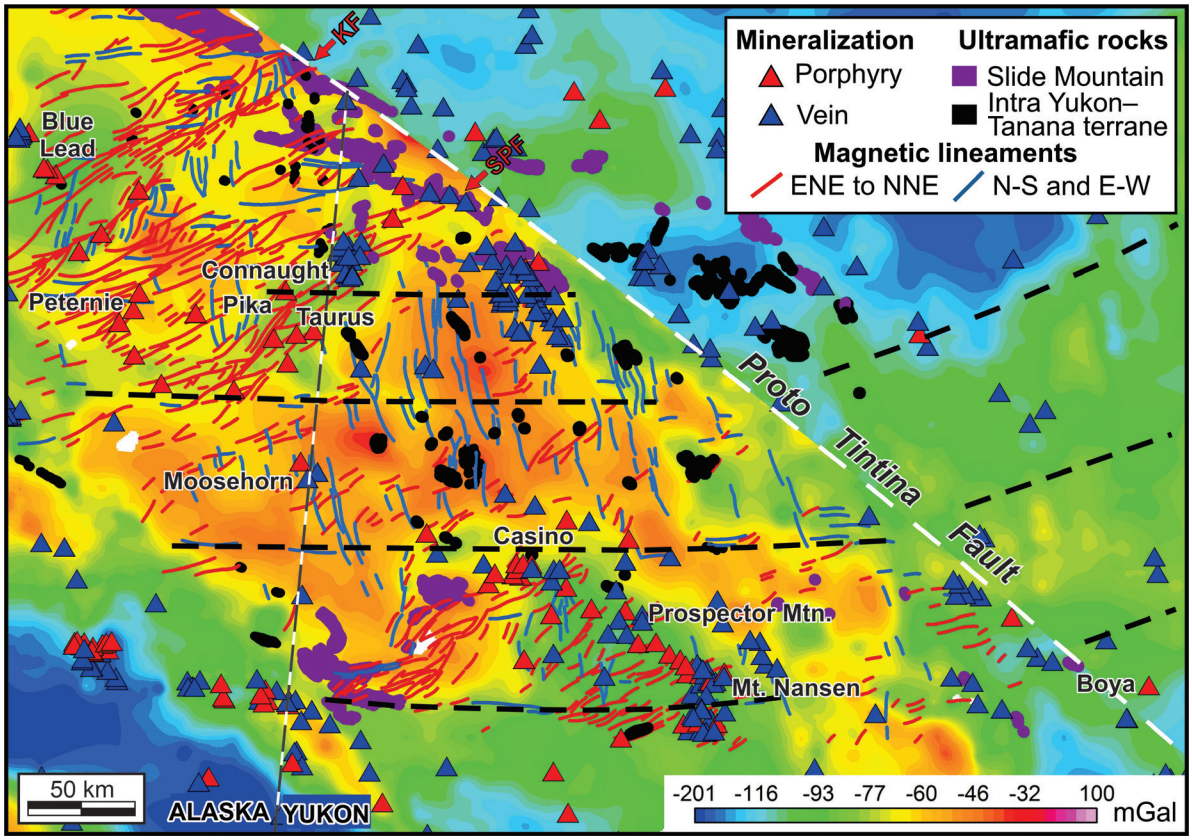

Figure 12. Relationship of crustal lineaments (heavy black dashed lines) to magnetic lineaments and mineral occurrence types and locations.

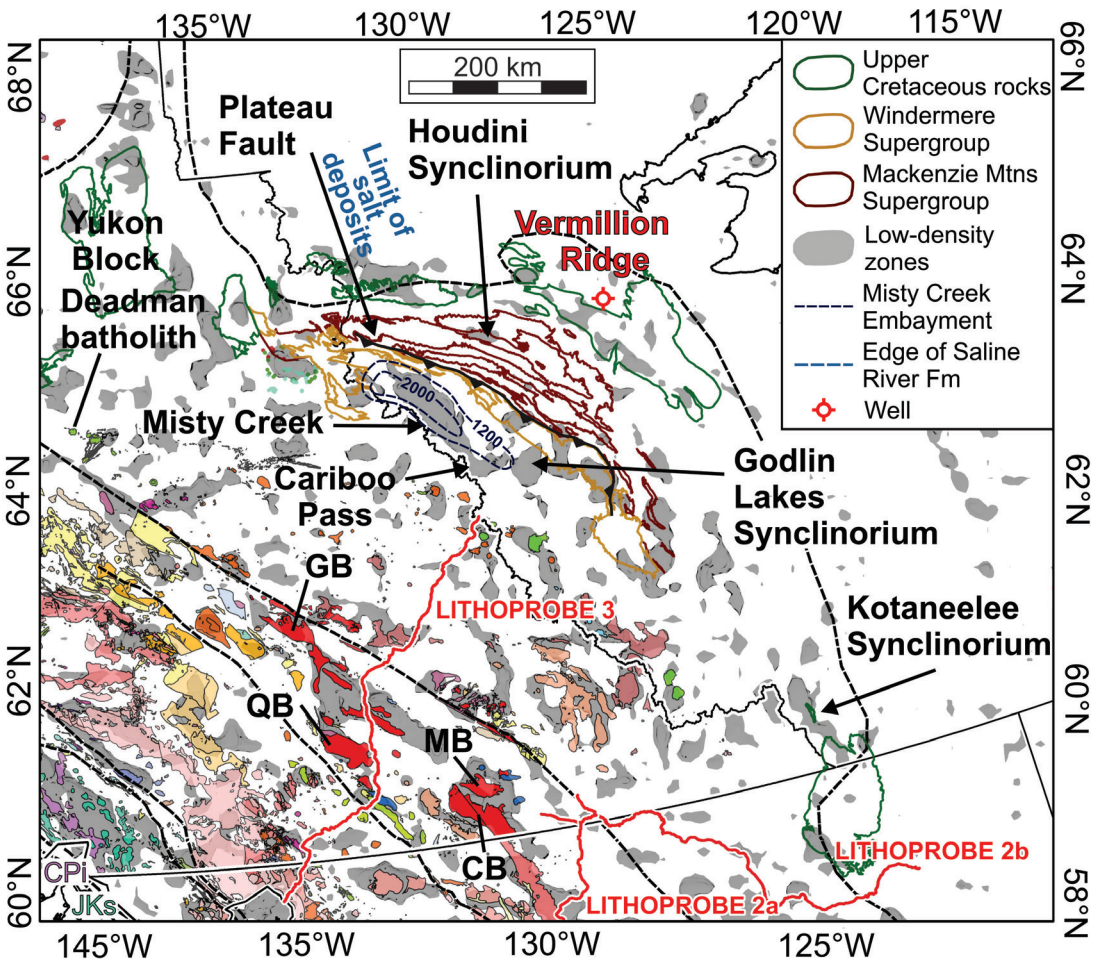

Figure 13. Relationship between low-density zones in the 3-D density model, to plutonic rocks of Yukon-Tanana terrane, Cassiar terrane, and Selwyn Basin, and Proterozoic and Cretaceous sedimentary rocks of the Mackenzie Mountains fold and thrust belt. CB = Cassiar batholith, GB = Glenlyon batholith, MB = Marker Lake batholith, QB = Quiet Lake batholith. Red lines show the location of LITHOPROBE seismic-reflection and -refraction profiles. For additional information on the geophysical and tectonic interpretation *see* Hayward (2019).

structural and stratigraphic information, and a focus on hydrocarbon exploration (e.g. Hayes, 2012). In 2004, two seismic-reflection lines were acquired for the Geological Survey of Canada by Kinetex Inc., across the sedimentary basin and adjacent terranes, in order to enhance the data set available for hydrocarbon assessments (e.g. Buffett et al., 2006).

The seismic data were reprocessed and reinterpreted (Calvert et al. 2017, Fig. 16a), with three-dimensional first-arrival tomographic inversion applied to constrain near-surface lithology and structure, enabling the correlation of the mapped bedrock geology (Fig. 15) to mid-crustal structures below. High-resolution (Yukon Geological Survey, 2011, 2012) and regional gravity data were inverted to 3-D density models. Density cross-sections (e.g. Fig. 16b), coincident with the seismic reflection profiles, were used to constrain structure and geological contacts in the seismic interpretation (e.g. Fig. 16a). Rocks of the Yukon-Tanana terrane are interpreted to extend beneath Quesnellia. The Stikinia and Quesnellia terranes underlie the Triassic to Early Cretaceous sedimentary rocks of the Whitehorse Trough and form a deep synform above the Yukon-Tanana terrane. Seismic-reflection geometries in the upper crust are complex, but are consistent with large-scale imbricate structures that have been dissected into numerous blocks by displacement along moderately to steeply dipping strike-slip faults, which may be part of a crustal-scale flower structure extending to the base of the crust (Fig. 16a).

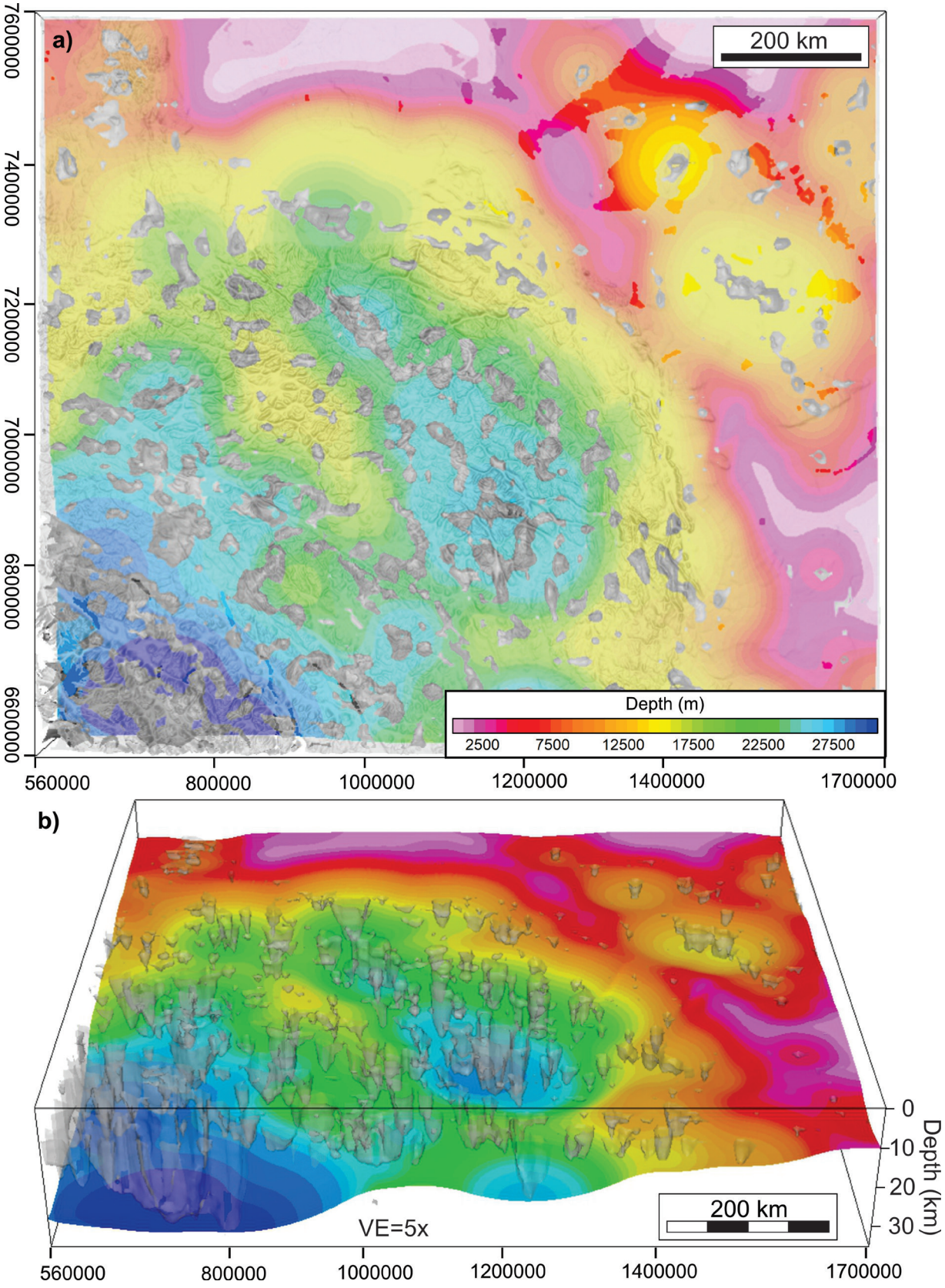

Figure 14. Low-density zones, within the 3-D density model from the inversion of Bouguer gravity data that constrain the depth of a crustal décollement (colour contours). **a)** View from above. **b)** Perspective view toward the north; 5x vertical exaggeration.

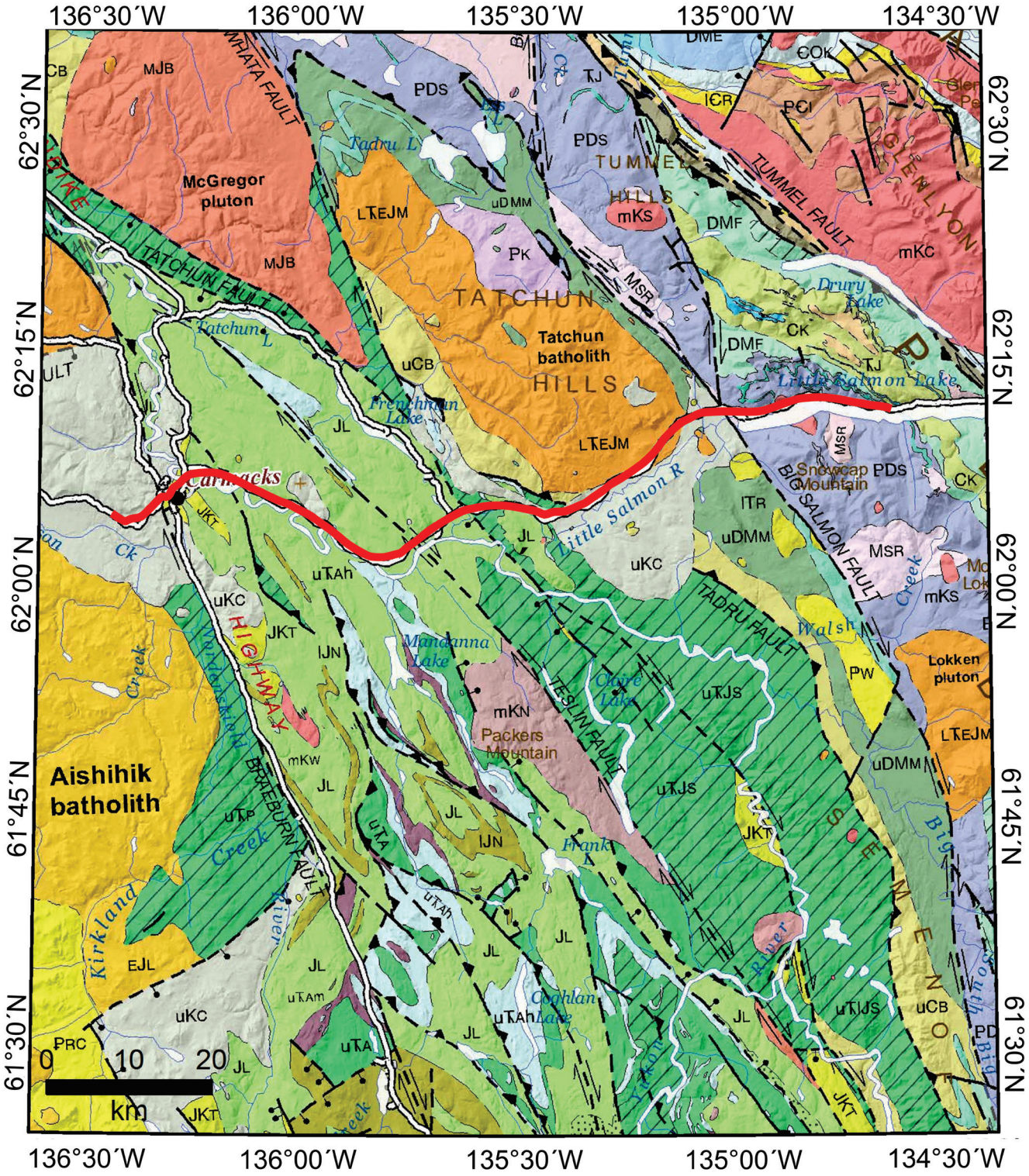

Figure 15. Geology of the northern Whitehorse trough (Yukon Geological Survey, 2018). Heavy red line shows the location of seismic-reflection profile shown in Figure 16, below.

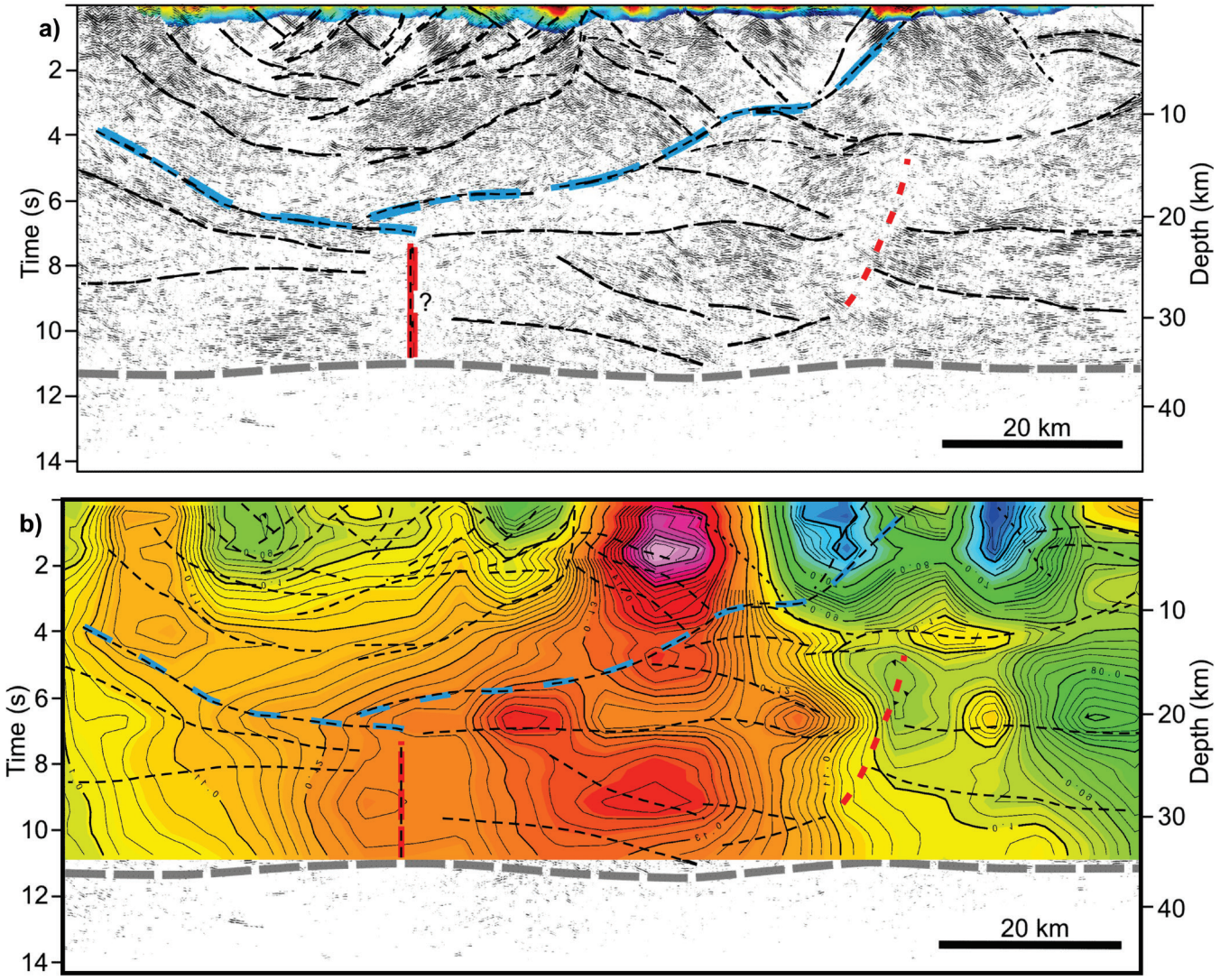

Figure 16. **a)** Preliminary interpretation of seismic-reflection data across the Whitehorse Trough. Black dashed lines show contacts and faults. Colour contours at the top of the section show the seismic P-wave velocity derived from first-arrival tomography. **b)** Section through the 3-D density model, derived from the 3-D inversion of high-resolution and regional Bouguer gravity data, illustrating the relationship between the seismically defined contacts and faults and crustal density variations.

Investigating the ancient course of northern Cordilleran rivers

The modern Yukon River flows to the north and drains a large drainage basin of central Yukon (Fig. 17). Previous studies have shown that the course of the Yukon River was modified from an originally southward-flowing direction by Pleistocene glaciations. Ryan et al. (2017) applied geophysical and hydrological modelling to investigate the impact of about 430 km of dextral displacement on the Tintina Fault, on the earlier development of the Yukon River and drainage basins of central Yukon. Wavelength filters, applied to topographic data (Fig. 17) from the northern Cordillera, highlight the largest river valleys (Fig. 18).

These images were incrementally restored for displacement on the Tintina Fault, and matches found visually for displacements where good alignment are identified between valleys and highlands across the fault (Fig. 18). At selected displacements, the potential historical course of the region's rivers was modelled (Fig. 19). The models show that the drainage of the Yukon River northwestward into Alaska was only possible at up to about 50–55 km restored displacement on the Tintina Fault (Fig. 19a, b). At large restored displacements of greater than 230 km (Fig. 19d), the models illustrate that paleo-Yukon River drainage may have flowed eastward into the continental interior via an ancestral Liard River. The revised drainage evolution has wide-reaching implications for the probable great antiquity of a landscape that has long been considered to be youthful, as well as the flow direction

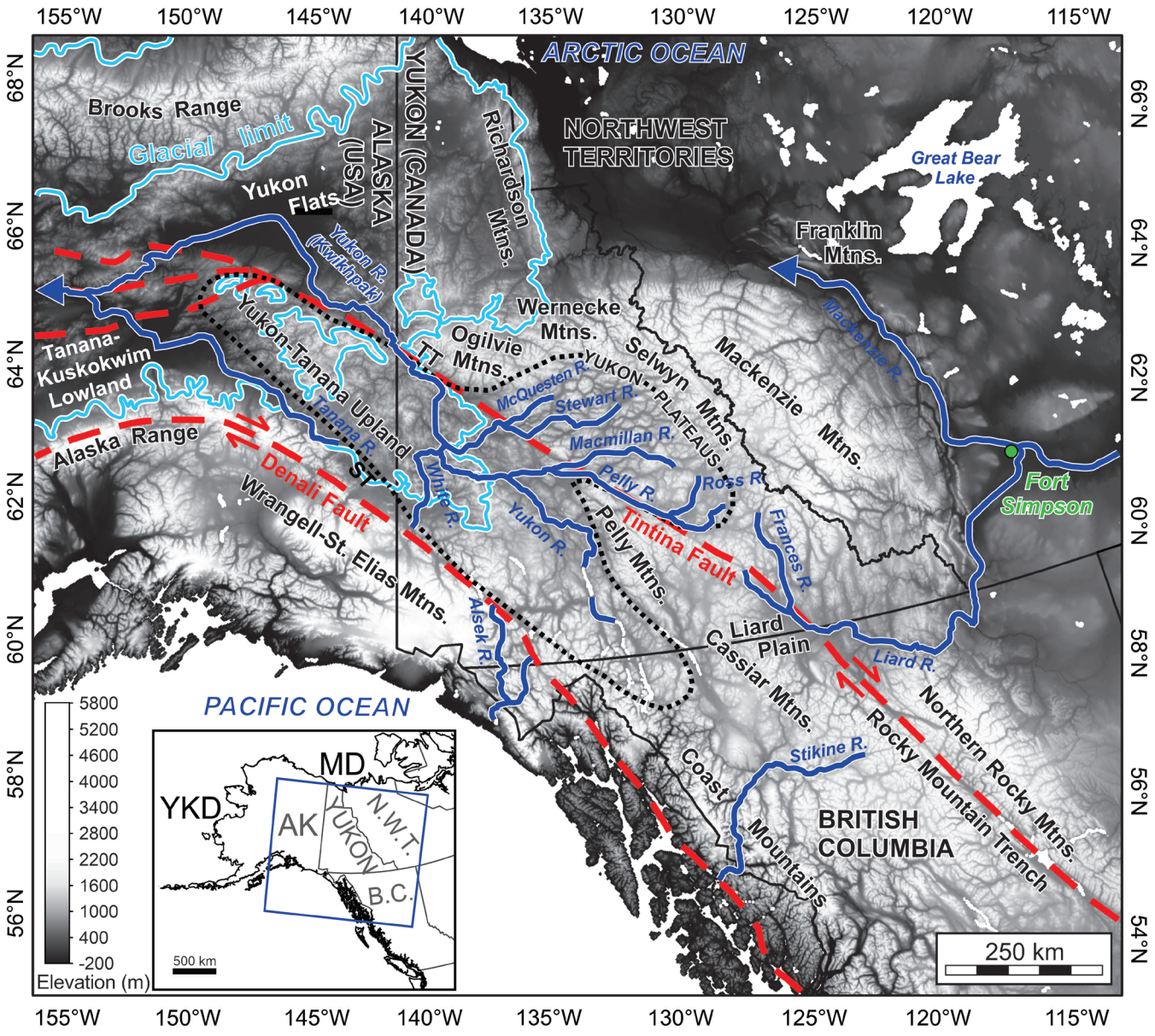

Figure 17. Topography and major rivers of the northern Cordillera (heavy dark blue lines). Heavy dashed red lines show major strike-slip faults. Light blue lines show the limits of Quaternary glaciations (Ryan et al., 2017); YKD = Yukon-Kuskokwim Delta, AK = Alaska, MD = Mackenzie Delta.

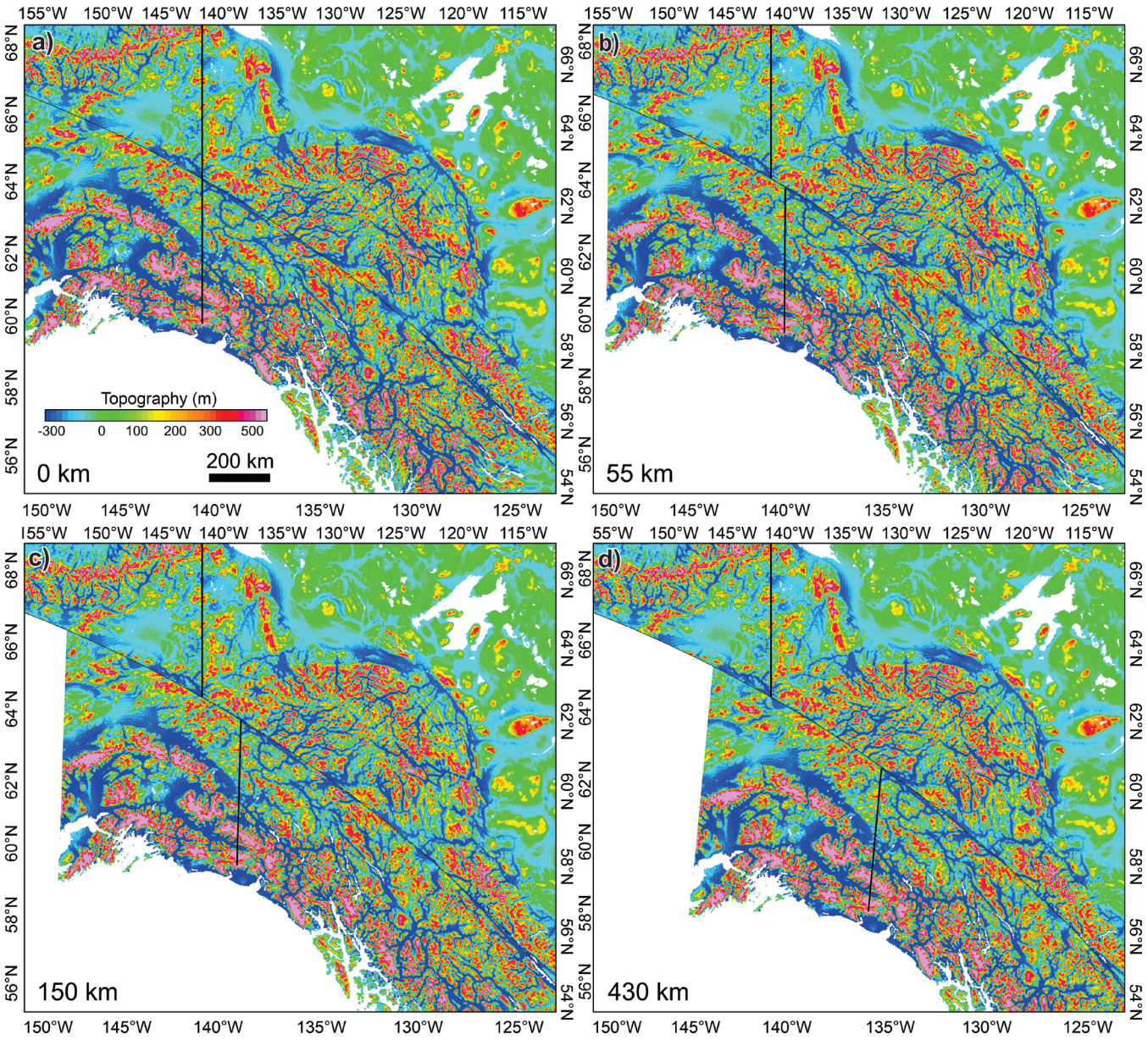

Figure 18. Filtered topographic data are incrementally restored for up to 430 km of right-lateral strike-slip displacement on the Tintina Fault, illustrating the alignments of topographic highs and valleys across the fault at different degrees of displacement **a)** 0 km, **b)** 55 km, **c)** 150 km, and **d)** 430 km of displacement.

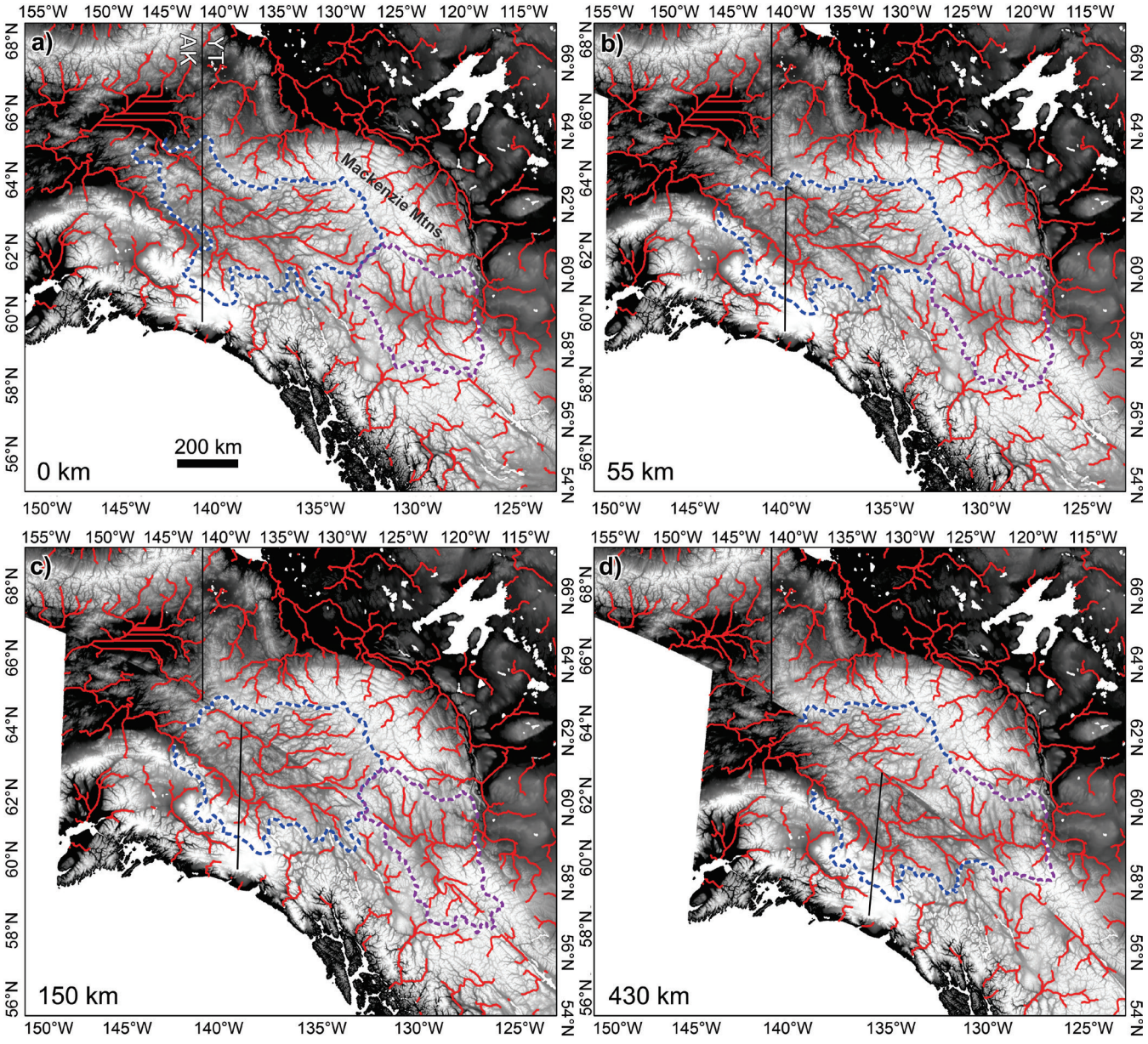

Figure 19. River drainage models for topographic data following restoration, in steps up to a maximum of 430 km, of right-lateral strike-slip displacement on the Tintina Fault. **a)** 0 km, **b)** 55 km, **c)** 150 km, **d)** 430 km, displacement as shown in figure 18. The blue-white dashed line shows the catchment of the Yukon River. The purple-white dashed line shows the catchment of the Liard River. Models suggest that at large restored displacements, the Yukon and Liard catchments may have merged and the rivers may have flowed toward the east (*see* Ryan et al. (2017) for discussion).

and channel geometries of the region's ancient rivers, and importantly, for exploration of surficial deposits including placer gold.

CONCLUSIONS

Geophysical data acquisition, analysis, interpretation, and modelling played a critical role in the research and enhanced understanding the geological and tectonic history of the northern Cordillera throughout the GEM Cordillera project. The data, which represent a large capital investment, have resulted in a comprehensive legacy data set of expansive high-resolution aeromagnetic coverage. Aeromagnetic data and interpretations, and regional data compilations, have been both welcomed and well used by GEM research scientists, and by provincial and territorial collaborators, and industry clients. The established best practice of data acquisition in an area prior to fieldwork is recommended for future programs in order to increase fieldwork efficiency and effectiveness, especially where large areas of Canadian territory are being mapped and evaluated with small teams of geologists. The new geophysical data have underpinned both local- and regional-scale research into the tectonic history of the Cordillera and are informing the development of future research programs.

REFERENCES

Boulanger, O. and Kiss, F., 2017a. Residual total magnetic field, aeromagnetic survey of the Llewellyn area, NTS 104-M/8 and parts of 104-M/1, 2, 6, 7, British Columbia; Geological Survey of Canada, Open File 8287, scale 1:100 000. https://doi.org/10.4095/305322

Boulanger, O. and Kiss, F., 2017b. Residual total magnetic field, aeromagnetic survey of the Llewellyn area, NTS 104-M/9, 10, 15, 16 and parts of 104-M/11, 14, British Columbia; Geological Survey of Canada, Open File 8288, scale 1:100 000. https://doi.org/10.4095/305323

Boulanger, O. and Kiss, F., 2017c. Residual total magnetic field, aeromagnetic survey of the Llewellyn area, NTS 105-D/1, 2, 3 and parts of 105-D/6, 7, 8, Yukon; Geological Survey of Canada, Open File 8289, scale 1:100 000. https://doi.org/10.4095/305324

Boulanger, O. and Kiss, F., 2017d. First vertical derivative of the magnetic field, aeromagnetic survey of the Llewellyn area, NTS 104-M/8 and parts of 104-M/1, 2, 6, 7, British Columbia; Geological Survey of Canada, Open File 8290, scale 1:100 000. https://doi.org/10.4095/305325

Boulanger, O. and Kiss, F., 2017e. First vertical derivative of the magnetic field, aeromagnetic survey of the Llewellyn area, NTS 104-M/9, 10, 15, 16 and parts of 104-M/11, 14, British Columbia; Geological Survey of Canada, Open File 8291, scale 1:100 000. https://doi.org/10.4095/305326

Boulanger, O. and Kiss, F., 2017f. First vertical derivative of the magnetic field, aeromagnetic survey of the Llewellyn area, NTS 105-D/1, 2, 3 and parts of 105-D/6, 7, 8, Yukon; Geological Survey of Canada, Open File 8292, scale 1:100 000. https://doi.org/10.4095/305327

Boulanger, O. and Kiss, F., 2018a. Residual total magnetic field, aeromagnetic survey of the Marsh Lake area, Yukon, part of NTS 105-C/south; Geological Survey of Canada, Open File 8412, scale 1:100 000. https://doi.org/10.4095/308223

Boulanger, O. and Kiss, F., 2018b. First vertical derivative of the magnetic field, aeromagnetic survey of the Marsh Lake area, Yukon, part of NTS 105-C/south; Geological Survey of Canada, Open File 8413, scale 1:100 000. https://doi.org/10.4095/308224

Boulanger, O. and Kiss, F., 2018c. Residual total magnetic field, aeromagnetic survey of the Marsh Lake area, Yukon, part of NTS 105-C/north; Geological Survey of Canada, Open File 8414, scale 1:100 000. https://doi.org/10.4095/308225

Boulanger, O. and Kiss, F., 2018d. First vertical derivative of the magnetic field, aeromagnetic survey of the Marsh Lake area, Yukon, part of NTS 105-C/north; Geological Survey of Canada, Open File 8415, scale 1:100 000. https://doi.org/10.4095/308226

Boulanger, O. and Kiss, F., 2018e. Residual total magnetic field, aeromagnetic survey of the Marsh Lake area, Yukon, part of NTS 105-D/south; Geological Survey of Canada, Open File 8416, scale 1:100 000. https://doi.org/10.4095/308227

Boulanger, O. and Kiss, F., 2018f. First vertical derivative of the magnetic field, aeromagnetic survey of the Marsh Lake area, Yukon, part of NTS 105-D/south; Geological Survey of Canada, Open File 8417, scale 1:100 000. https://doi.org/10.4095/308228

Boulanger, O. and Kiss, F., 2018g. Residual total magnetic field, aeromagnetic survey of the Marsh Lake area, Yukon, part of NTS 105-D/north; Geological Survey of Canada, Open File 8418, scale 1:100 000. https://doi.org/10.4095/308229

Boulanger, O. and Kiss, F., 2018h. First vertical derivative of the magnetic field, aeromagnetic survey of the Marsh Lake area, Yukon, part of NTS 105-D/north; Geological Survey of Canada, Open File 8419, scale 1:100 000. https://doi.org/10.4095/308230

Braun, J., 2016. Strong imprint of past orogenic events on the thermochronological record; Tectonophysics, v. 683, p. 325–332. https://doi.org/10.1016/j.tecto.2016.05.046

Buffett, G., White, D., Roberts, B., and Colpron, M., 2006. Preliminary results from the Whitehorse Trough seismic survey, Yukon Territory; Geological Survey of Canada, Current Research 2006-A2, 9 p. https://doi.org/10.4095/221662

Calvert, A.J., Hayward, N., Vayavur, R., and Colpron, M., 2017. Seismic and gravity constraints on the crustal architecture of the Intermontane terranes, central Yukon; Canadian Journal of Earth Sciences, v. 54, p. 798–811. https://doi.org/10.1139/cjes-2016-0189

Carson, J.M., Dumont, R., and Harvey, B.J.A., 2009a. Geophysical Series, NTS 115 K/1, airborne geophysical survey southern Stevenson Ridge area, Yukon / Série des cartes géophysiques, SNRC 115 K/1, levé géophysique aéroporté région de Stevenson Ridge sud, Yukon; Geological Survey of Canada, Open File 6127, scale 1:50 000. https://doi.org/10.4095/247677

Carson, J.M., Dumont, R., and Harvey, B.J.A., 2009b. Geophysical Series, NTS 115 J/4, airborne geophysical survey southern Stevenson Ridge area, Yukon / Série des cartes géophysiques, SNRC 115 J/4, levé géophysique aéroporté région de Stevenson Ridge sud, Yukon. Geological Survey of Canada, Open File 6128, scale 1:50 000. https://doi.org/10.4095/247679

Carson, J.M., Dumont, R., and Harvey, B.J.A., 2009c. Geophysical Series, NTS 115 J/3, airborne geophysical survey southern Stevenson Ridge area, Yukon / Série des cartes géophysiques, SNRC 115 J/3, levé géophysique aéroporté région de Stevenson Ridge sud, Yukon; Geological Survey of Canada, Open File 6129, scale 1:50 000. https://doi.org/10.4095/247680

Cleven, N.R., Ryan, J.J., Zagorevski, A., and Hayward, N., 2018. Revised tectonostratigraphy of Yukon Tanana and Slide Mountain terrane units in the Thirtymile Range and Wolf Lake areas, southern Yukon: GEM-2 Cordillera project, report of activities 2018; Geological Survey of Canada, Open File 8476, 13 p. https://doi.org/10.4095/311323

Colpron, M. and Nelson, J.L., 2011. A Digital Atlas of Terranes for the northern Cordillera; Yukon Geological Survey. <http://www.geology.gov.yk.ca> [accessed March 12, 2014]

Cook, T., 2019. Resolving a Cordilleran Conundrum; Eos, Research Spotlight, American Geophysical Union. <https://eos.org/research-spotlights/resolving-a-cordilleran-conundrum> [accessed March 15, 2019]

Geological Survey of Canada, 2019a. Geoscience Data Repository for Geophysical Data, Gravity, Point Data; Natural Resources Canada. <http://gdr.agg.nrcan.gc.ca/gdrdap/dap/searcheng.php1> [accessed May 15, 2019]

Geological Survey of Canada, 2019b. Geoscience Data Repository for Geophysical Data, Magnetic-Radiometric-EM, Compilations, Canada-200m-MAG, Natural Resources Canada. <http://gdr.agg.nrcan.gc.ca/gdrdap/dap/searcheng.php1> [accessed May 15, 2019].

Hayes, B.J.R., 2012. Petroleum resource assessment of Whitehorse trough, Yukon, Canada; Yukon Geological Survey, Miscellaneous Report 6, 52 p.

Hayward, N., 2015. Geophysical investigation and reconstruction of lithospheric structure and its control on geology, structure, and mineralization in the Cordillera of northern Canada and eastern Alaska; Tectonics, v. 34, p. 2165–2189. https://doi.org/10.1002/2015TC003871

Hayward, N., 2019. The 3D geophysical investigation of a Middle Cretaceous to Paleocene regional décollement in the Cordillera of northern Canada and Alaska; Tectonics, v. 38, p. 307–334. https://doi.org/10.1029/2018TC005295

Hayward, N., Miles, W., and Oneschuk, D., 2011a. Geophysical Series, detailed geophysical compilation project, Yukon Plateau, Yukon, NTS 115-I, J, K, N, O, P and 116A and B / Série des cartes géophysiques, projet de compilation géophysique détaillée, Plateau du Yukon, Yukon, SNRC 115-I, J, K, N, O, P et 116A et B; Geological Survey of Canada, Open File 6958, scale 1:350 000. https://doi.org/10.4095/289240

Hayward, N., Miles, W., and Oneschuk, D., 2011b. Geophysical Series, regional geophysical compilation project, Yukon Plateau, Yukon, parts of NTS 105, 106, 115 and 116 / Série des cartes géophysiques, projet de compilation géophysique régionale, Plateau du Yukon, Yukon, SNRC parties de 105, 106, 115 et 116; Geological Survey of Canada, Open File 6959, scale 1:750 000. https://doi.org/10.4095/289241

Hayward, N., Miles, W., and Oneschuk, D., 2012. Geophysical Series, detailed geophysical compilation project, Yukon Plateau, Yukon, NTS 115-I, J, K, N, O, P and 116A and B / Série des cartes géophysiques, projet de compilation géophysique détaillée, Plateau du Yukon, Yukon, SNRC 115-I, J, K, N, O, P et 116A et B; Geological Survey of Canada, Open File 7279, scale 1:350 000. https://doi.org/10.4095/292097

Israel, S., Cobbett, R., Westberg, E., Stanley, B., and Hayward, N., 2011. Preliminary bedrock geology map of the Ruby Ranges, southwest Yukon (Parts of NTS 115G, 115H, 115A and 115B); Yukon Geological Survey, Open File 2011-2, scale 1:150 000.

Kellett, D.A., Ryan, J.J., Colpron, M., Zagorevski, A., Joyce, N., and Zwingmann, H., 2017. Report of activities, 2017, for Yukon tectonic evolution – late Mesozoic to Tertiary: GEM2 Cordillera Project; Geological Survey of Canada, Open File 8306, 14 p. https://doi.org/10.4095/305956

Kellett, D.A., Mottram, C., Banjan, M., Coutand, I., and Friend, M., 2018. Yukon tectonic evolution – late Mesozoic to Tertiary: GEM-2 Cordillera Project, report of activities 2018; Geological Survey of Canada, Open File 8470, 14 p. https://doi.org/10.4095/311263

Kiss, F., 2010a. Residual total magnetic field, Kluane area aeromagnetic survey, parts of NTS 115 A/13, 115 A/14 and 115 B/16, Yukon / Composante résiduelle du champ magnétique total, levé aéromagnétique de la région de Kluane, SNRC parties de 115 A/13, 115 A/14 et 115 B/16, Yukon; Geological Survey of Canada, Open File 6584, scale 1:50 000. https://doi.org/10.4095/286068

Kiss, F., 2010b. First vertical derivative of the magnetic field, Kluane area aeromagnetic survey, parts of NTS 115 A/13, 115 A/14 and 115 B/16, Yukon / Dérivée première verticale du champ magnétique, levé aéromagnétique de la région de Kluane, SNRC parties de 115 A/13, 115 A/14 et 115 B/16, Yukon; Geological Survey of Canada, Open File 6585, scale 1:50 000. https://doi.org/10.4095/286069

Kiss, F., 2010c. Residual total magnetic field, Kluane area aeromagnetic survey, NTS 115 H/4 and parts of 115 H/3 and 115 G/1, Yukon / Composante résiduelle du champ magnétique total, levé aéromagnétique de la région de Kluane, SNRC 115 H/4 et parties de 115 H/3 et 115 G/1, Yukon; Geological Survey of Canada, Open File 6586, scale 1:50 000. https://doi.org/10.4095/286070

Kiss, F., 2010d. First vertical derivative of the magnetic field, Kluane area aeromagnetic survey, NTS 115 H/4 and parts of 115 H/3 and 115 G/1, Yukon / Dérivée première verticale du champ magnétique, levé aéromagnétique de la région de Kluane, SNRC 115 H/4 et parties de 115 H/3 et 115 G/1, Yukon; Geological Survey of Canada, Open File 6587, scale 1:50 000. https://doi.org/10.4095/286071

Kiss, F., 2010e. Residual total magnetic field, Kluane area aeromagnetic survey, parts of NTS 115 G/8, 115 H/5 and 115 H/6, Yukon / Composante résiduelle du champ magnétique total, levé aéromagnétique de la région de Kluane, SNRC parties de 115 G/8, 115 H/5 et 115 H/6, Yukon; Geological Survey of Canada, Open File 6588, scale 1:50 000. https://doi.org/10.4095/286072

Kiss, F., 2010f. First vertical derivative of the magnetic field, Kluane area aeromagnetic survey, parts of NTS 115 G/8, 115 H/5 and 115 H/6, Yukon / Dérivée première verticale du champ magnétique, levé aéromagnétique de la région de Kluane, SNRC parties de 115 G/8, 115 H/5 and 115 H/6, Yukon; Geological Survey of Canada, Open File 6589, scale 1:50 000. https://doi.org/10.4095/286073

Kiss, F., 2010g. Residual total magnetic field, Kluane area aeromagnetic survey, parts of NTS 115 H/11 and 115 H/12, Yukon / Composante résiduelle du champ magnétique total, levé aéromagnétique de la région de Kluane, SNRC parties de 115 H/11 et 115 H/12, Yukon; Geological Survey of Canada, Open File 6590, scale 1:50 000. https://doi.org/10.4095/286074

Kiss, F., 2010h. First vertical derivative of the magnetic field, Kluane area aeromagnetic survey, parts of NTS 115 H/11 and 115 H/12, Yukon / Dérivée première verticale du champ magnétique, levé aéromagnétique de la région de Kluane, SNRC parties de 115 H/11 et 115 H/12, Yukon; Geological Survey of Canada, Open File 6591, scale 1:50 000. https://doi.org/10.4095/286075

Kiss, F., 2012a. Residual total magnetic field, aeromagnetic survey of the Scroggie Creek and Wolverine Creek areas, NTS 115-I/11 and parts of NTS 115-I/5, 6, 12, Yukon / Composante résiduelle du champ magnétique total, levé aéromagnétique des régions du ruisseau Scroggie et du ruisseau Wolverine, SNRC 115-I/11 et parties de 115-I/5, 6, 12, Yukon; Geological Survey of Canada, Open File 7177, scale 1:50 000. https://doi.org/10.4095/292022

Kiss, F., 2012b. First vertical derivative of the magnetic field, aeromagnetic survey of the Scroggie Creek and Wolverine Creek areas, NTS 115-I/11 and parts of NTS 115-I/5, 6, 12, Yukon / Dérivée première verticale du champ magnétique, levé aéromagnétique des régions du ruisseau Scroggie et du ruisseau Wolverine, SNRC 115-I/11 et parties de 115-I/5, 6, 12, Yukon; Geological Survey of Canada, Open File 7178, scale 1:50 000. https://doi.org/10.4095/292023

Kiss, F., 2012c. Residual total magnetic field, aeromagnetic survey of the Scroggie Creek and Wolverine Creek areas, NTS 115-O/2 and part of 115-O/3, Yukon / Composante résiduelle du champ magnétique total, levé aéromagnétique des régions du ruisseau Scroggie et du ruisseau Wolverine, SNRC 115-O/2 et partie de 115-O/3, Yukon; Geological Survey of Canada, Open File 7179, scale 1:50 000. https://doi.org/10.4095/292024

Kiss, F., 2012d. First vertical derivative of the magnetic field, aeromagnetic survey of the Scroggie Creek and Wolverine Creek areas, NTS 115-O/2 and part of 115-O/3, Yukon / Dérivée première verticale du champ magnétique, levé aéromagnétique des régions du ruisseau Scroggie et du ruisseau Wolverine, SNRC 115-O/2 et partie de 115-O/3, Yukon; Geological Survey of Canada, Open File 7180, scale 1:50 000. https://doi.org/10.4095/292025

Kiss, F., 2012e. Residual total magnetic field, aeromagnetic survey of the Scroggie Creek and Wolverine Creek areas, NTS 115-O/4 and part of 115-O/3, Yukon / Composante résiduelle du champ magnétique total, levé aéromagnétique des régions du ruisseau Scroggie et du ruisseau Wolverine, SNRC 115-O/4 et partie de 115-O/3, Yukon; Geological Survey of Canada, Open File 7181, scale 1:50 000. https://doi.org/10.4095/292026

Kiss, F., 2012f. First vertical derivative of the magnetic field, aeromagnetic survey of the Scroggie Creek and Wolverine Creek areas, NTS 115-O/4 and part of 115-O/3, Yukon / Dérivée première verticale du champ magnétique, levé aéromagnétique des régions du ruisseau Scroggie et du ruisseau Wolverine, SNRC 115-O/4 et partie de 115-O/3, Yukon; Geological Survey of Canada, Open File 7182, scale 1:50 000. https://doi.org/10.4095/292027

Kiss, F., 2012g. Residual total magnetic field, aeromagnetic survey of the Scroggie Creek and Wolverine Creek areas, NTS 115-O/6 and part of 115-O/7, Yukon / Composante résiduelle du champ magnétique total, levé aéromagnétique des régions du ruisseau Scroggie et du ruisseau Wolverine, SNRC 115-O/6 et partie de 115-O/7, Yukon; Geological Survey of Canada, Open File 7183, scale 1:50 000. https://doi.org/10.4095/292028

Kiss, F., 2012h. First vertical derivative of the magnetic field, aeromagnetic survey of the Scroggie Creek and Wolverine Creek areas, NTS 115-O/6 and part of 115-O/7, Yukon / Dérivée première verticale du champ magnétique, levé aéromagnétique des régions du ruisseau Scroggie et du ruisseau Wolverine, SNRC 115-O/6 et partie de 115-O/7, Yukon; Geological Survey of Canada, Open File 7184, scale 1:50 000. https://doi.org/10.4095/292029

Kiss, F., 2012i. Residual total magnetic field, aeromagnetic survey of the Scroggie Creek and Wolverine Creek areas, NTS 115-O/8 and part of 115-O/7, Yukon / Composante résiduelle du champ magnétique total, levé aéromagnétique des régions du ruisseau Scroggie et du ruisseau Wolverine, SNRC 115-O/8 et partie de 115-O/7, Yukon; Geological Survey of Canada, Open File 7185, scale 1:50 000. https://doi.org/10.4095/292030

Kiss, F., 2012j. First vertical derivative of the magnetic field, aeromagnetic survey of the Scroggie Creek and Wolverine Creek areas, NTS 115-O/8 and part of 115-O/7, Yukon / Dérivée première verticale du champ magnétique, levé aéromagnétique des régions du ruisseau Scroggie et du ruisseau Wolverine, SNRC 115-O/8 et partie de 115-O/7, Yukon; Geological Survey of Canada, Open File 7186, scale 1:50 000. https://doi.org/10.4095/292031

Kiss, F., 2012k. Residual total magnetic field, aeromagnetic survey of the Scroggie Creek and Wolverine Creek areas, NTS 115-O/9 and part of NTS 115-O/10, Yukon / Composante résiduelle du champ magnétique total, levé aéromagnétique des régions du ruisseau Scroggie et du ruisseau Wolverine, SNRC 115-O/9 et partie de 115-O/10, Yukon; Geological Survey of Canada, Open File 7187, scale 1:50 000. https://doi.org/10.4095/292032

Kiss, F., 2012l. First vertical derivative of the magnetic field, aeromagnetic survey of the Scroggie Creek and Wolverine Creek areas, NTS 115-O/9 and part of NTS 115-O/10, Yukon / Dérivée première verticale du champ magnétique, levé aéromagnétique des régions du ruisseau Scroggie et du ruisseau Wolverine, SNRC 115-O/9 et partie de 115-O/10, Yukon; Geological Survey of Canada, Open File 7188, scale 1:50 000. https://doi.org/10.4095/292033

Kiss, F., 2012m. Residual total magnetic field, aeromagnetic survey of the Scroggie Creek and Wolverine Creek areas, NTS 115-P/12 and part of 115-P/11, Yukon / Composante résiduelle du champ magnétique total, levé aéromagnétique des régions du ruisseau Scroggie et du ruisseau Wolverine, SNRC 115-P/12 et partie de 115-P/11, Yukon; Geological Survey of Canada, Open File 7189, scale 1:50 000. https://doi.org/10.4095/292034

Kiss, F., 2012n. First vertical derivative of the magnetic field, aeromagnetic survey of the Scroggie Creek and Wolverine Creek areas, NTS 115-P/12 and part of 115-P/11, Yukon / Dérivée première verticale du champ magnétique, levé aéromagnétique des régions du ruisseau Scroggie et du ruisseau Wolverine, SNRC 115-P/12 et partie de 115-P/11, Yukon; Geological Survey of Canada, Open File 7190, scale 1:50 000. https://doi.org/10.4095/292035

Kiss, F., 2012o. Residual total magnetic field, aeromagnetic survey of the Scroggie Creek and Wolverine Creek areas, NTS 115-P/13 and part of NTS 115-P/14, Yukon / Composante résiduelle du champ magnétique total, levé aéromagnétique des régions du ruisseau Scroggie et du ruisseau Wolverine, SNRC 115-P/13 et partie de 115-P/14, Yukon; Geological Survey of Canada, Open File 7191, scale 1:50 000. https://doi.org/10.4095/292036

Kiss, F., 2019a. Residual total magnetic field, aeromagnetic survey of the Wolf Lake area, Yukon, part of NTS 105-F (south half); Geological Survey of Canada, Open File 8601, scale 1:100 000. https://doi.org/10.4095/314827

Kiss, F., 2019b. First vertical derivative of the magnetic field, aeromagnetic survey of the Wolf Lake area, Yukon, part of NTS 105-F (south half); Geological Survey of Canada, Open File 8602, scale 1:100 000. https://doi.org/10.4095/314828

Kiss, F., 2019c. Residual total magnetic field, aeromagnetic survey of the Wolf Lake area, Yukon, part of NTS 105-G (south half); Geological Survey of Canada, Open File 8603, scale 1:100 000. https://doi.org/10.4095/314829

Kiss, F., 2019d. First vertical derivative of the magnetic field, aeromagnetic survey of the Wolf Lake area, Yukon, part of NTS 105-G (south half); Geological Survey of Canada, Open File 8604, scale 1:100 000. https://doi.org/10.4095/314831

Kiss, F., 2019e. Residual total magnetic field, aeromagnetic survey of the Wolf Lake area, Yukon, part of NTS 105-C (north half); Geological Survey of Canada, Open File 8605, scale 1:100 000. https://doi.org/10.4095/314832

Kiss, F., 2019f. First vertical derivative of the magnetic field, aeromagnetic survey of the Wolf Lake area, Yukon, part of NTS 105-C (north half); Geological Survey of Canada, Open File 8606, scale 1:100 000. https://doi.org/10.4095/314833

Kiss, F., 2019g. Residual total magnetic field, aeromagnetic survey of the Wolf Lake area, Yukon, part of NTS 105-B (north half); Geological Survey of Canada, Open File 8607, scale 1:100 000. https://doi.org/10.4095/314834

Kiss, F., 2019h. First vertical derivative of the magnetic field, aeromagnetic survey of the Wolf Lake area, Yukon, part of NTS 105-B (north half); Geological Survey of Canada, Open File 8608, scale 1:100 000. https://doi.org/10.4095/314836

Kiss, F., 2019i. Residual total magnetic field, aeromagnetic survey of the Wolf Lake area, Yukon, part of NTS 105-B (south half) and 105-C (south half); Geological Survey of Canada, Open File 8609, scale 1:100 000. https://doi.org/10.4095/314837

Kiss, F., 2019j. First vertical derivative of the magnetic field, aeromagnetic survey of the Wolf Lake area, Yukon, part of NTS 105-B (south half) and 105-C (south half); Geological Survey of Canada, Open File 8610, scale 1:100 000. https://doi.org/10.4095/314838

Kiss, F., 2019k. Residual total magnetic field, aeromagnetic survey of the Wolf Lake area, Yukon, part of NTS 105-B (south half); Geological Survey of Canada, Open File 8611, scale 1:100 000. https://doi.org/10.4095/314839

Kiss, F., 2019l. First vertical derivative of the magnetic field, aeromagnetic survey of the Wolf Lake area, Yukon, part of NTS 105-B (south half); Geological Survey of Canada, Open File 8612, scale 1:100 000. https://doi.org/10.4095/314840

Kiss, F. and Boulanger, O., 2016a. Residual total magnetic field, aeromagnetic survey of the Frances Lake area, Yukon, NTS 105-A/10 and parts of NTS 105-A/6, 7, 9, 11; Geological Survey of Canada, Open File 8063, scale 1:100 000. https://doi.org/10.4095/298678

Kiss, F. and Boulanger, O., 2016b. First vertical derivative of the magnetic field, aeromagnetic survey of the Frances Lake area, Yukon, NTS 105-A/10 and parts of NTS 105-A/6, 7, 9, 11; Geological Survey of Canada, Open File 8064, scale 1:100 000. https://doi.org/10.4095/298679

Kiss, F. and Boulanger, O., 2016c. Residual total magnetic field, aeromagnetic survey of the Frances Lake area, Yukon, NTS 105-A/15 and parts of NTS 105-A/14, 16, H/2, 3, 4; Geological Survey of Canada, Open File 8065, scale 1:100 000. https://doi.org/10.4095/298680

Kiss, F. and Boulanger, O., 2016d. First vertical derivative of the magnetic field, aeromagnetic survey of the Frances Lake area, Yukon, NTS 105-A/15 and parts of NTS 105-A/14, 16, H/2, 3, 4; Geological Survey of Canada, Open File 8066, scale 1:100 000. https://doi.org/10.4095/298681

Kiss, F. and Boulanger, O., 2016e. Residual total magnetic field, aeromagnetic survey of the Frances Lake area, Yukon, NTS 105-H/6, 12 and parts of 105-G/9, H/5, 7, 10, 11; Geological Survey of Canada, Open File 8067, scale 1:100 000. https://doi.org/10.4095/298682

Kiss, F. and Boulanger, O., 2016f. First vertical derivative of the magnetic field, aeromagnetic survey of the Frances Lake area, Yukon, NTS 105-H/6, 12 and parts of 105-G/9, H/5, 7, 10, 11; Geological Survey of Canada, Open File 8068, scale 1:100 000. https://doi.org/10.4095/298683

Kiss, F. and Boulanger, O., 2016g. Residual total magnetic field, aeromagnetic survey of the Frances Lake area, Yukon, NTS 105-G/16 and parts of 105-G/15, H/13, 14, I/4, J/1, 2; Geological Survey of Canada, Open File 8069, scale 1:100 000. https://doi.org/10.4095/298684

Kiss, F. and Boulanger, O., 2016h. First vertical derivative of the magnetic field, aeromagnetic survey of the Frances Lake area, Yukon, NTS 105-G/16 and parts of 105-G/15, H/13, 14, I/4, J/1, 2; Geological Survey of Canada, Open File 8070, scale 1:100 000. https://doi.org/10.4095/298685

Kiss, F. and Boulanger, O., 2018a. Residual total magnetic field, aeromagnetic survey of the Marsh Lake area, Yukon, part of NTS 105-C/south; Geological Survey of Canada, Open File 8412, scale 1:100 000. https://doi.org/10.4095/308223

Kiss, F. and Boulanger, O., 2018b. First vertical derivative of the magnetic field, aeromagnetic survey of the Marsh Lake area, Yukon, part of NTS 105-C/south; Geological Survey of Canada, Open File 8413, scale 1:100 000. https://doi.org/10.4095/308224

Kiss, F. and Boulanger, O., 2018c. Residual total magnetic field, aeromagnetic survey of the Marsh Lake area, Yukon, part of NTS 105-C/north; Geological Survey of Canada, Open File 8414, scale 1:100 000. https://doi.org/10.4095/308225

Kiss, F. and Boulanger, O., 2018d. First vertical derivative of the magnetic field, aeromagnetic survey of the Marsh Lake area, Yukon, part of NTS 105-C/north; Geological Survey of Canada, Open File 8415, scale 1:100 000. https://doi.org/10.4095/308226

Kiss, F. and Boulanger, O., 2018e. Residual total magnetic field, aeromagnetic survey of the Marsh Lake area, Yukon, part of NTS 105-D/south; Geological Survey of Canada, Open File 8416, scale 1:100 000. https://doi.org/10.4095/308227

Kiss, F. and Boulanger, O., 2018f. First vertical derivative of the magnetic field, aeromagnetic survey of the Marsh Lake area, Yukon, part of NTS 105-D/south; Geological Survey of Canada, Open File 8417, scale 1:100 000. https://doi.org/10.4095/308228

Kiss, F. and Boulanger, O., 2018g. Residual total magnetic field, aeromagnetic survey of the Marsh Lake area, Yukon, part of NTS 105-D/north; Geological Survey of Canada, Open File 8418, scale 1:100 000. https://doi.org/10.4095/308229

Kiss, F. and Boulanger, O., 2018h. First vertical derivative of the magnetic field, aeromagnetic survey of the Marsh Lake area, Yukon, part of NTS 105-D/north; Geological Survey of Canada, Open File 8419, scale 1:100 000. https://doi.org/10.4095/308230

Kiss, F. and Boulanger, O., 2018i. Residual total magnetic field, aeromagnetic survey of the Marsh Lake area, Yukon, part of NTS 105-E/south; Geological Survey of Canada, Open File 8420, scale 1:100 000. https://doi.org/10.4095/308231

Kiss, F. and Boulanger, O., 2018j. First vertical derivative of the magnetic field, aeromagnetic survey of the Marsh Lake area, Yukon, part of NTS 105-E/south; Geological Survey of Canada, Open File 8421, scale 1:100 000. https://doi.org/10.4095/308232

Kiss, F. and Boulanger, O., 2018k. Residual total magnetic field, aeromagnetic survey of the Marsh Lake area, Yukon, part of NTS 105-E/north; Geological Survey of Canada, Open File 8422, scale 1:100 000. https://doi.org/10.4095/308233

Kiss, F. and Boulanger, O., 2018l. First vertical derivative of the magnetic field, aeromagnetic survey of the Marsh Lake area, Yukon, part of NTS 105-E/north; Geological Survey of Canada, Open File 8423, scale 1:100 000. https://doi.org/10.4095/308234

Kiss, F. and Boulanger, O., 2018m. Residual total magnetic field, aeromagnetic survey of the Marsh Lake area, Yukon, part of NTS 105-F/south; Geological Survey of Canada, Open File 8424, scale 1:100 000. https://doi.org/10.4095/308235

Kiss, F. and Boulanger, O., 2018n. First vertical derivative of the magnetic field, aeromagnetic survey of the Marsh Lake area, Yukon, part of NTS 105-F/south; Geological Survey of Canada, Open File 8425, scale 1:100 000. https://doi.org/10.4095/308236

Kiss, F. and Boulanger, O., 2018o. Residual total magnetic field, aeromagnetic survey of the Marsh Lake area, Yukon, part of NTS 105-F/north; Geological Survey of Canada, Open File 8426, scale 1:100 000. https://doi.org/10.4095/308237

Kiss, F. and Coyle, M., 2009a. Residual total magnetic field, McQuesten aeromagnetic survey, NTS 115-I/13 and 115-I/14, Yukon / Composante résiduelle du champ magnétique total, levé aéromagnétique McQuesten, SNRC 115-I/13 et 115-I/14, Yukon; Geological Survey of Canada, Open File 6106, scale 1:50 000. https://doi.org/10.4095/247494

Kiss, F. and Coyle, M., 2009b. First vertical derivative of the magnetic field, McQuesten aeromagnetic survey, NTS 115-I/13 and 115-I/14, Yukon / Dérivée première verticale du champ magnétique, levé aéromagnétique McQuesten, SNRC 115-I/13 et 115-I/14, Yukon; Geological Survey of Canada, Open File 6107, scale 1:50 000. https://doi.org/10.4095/247495

Kiss, F. and Coyle, M., 2009c. Residual total magnetic field, McQuesten aeromagnetic survey, NTS 115-I/15, Yukon / Composante résiduelle du champ magnétique total, levé aéromagnétique McQuesten, SNRC 115-I/15, Yukon; Geological Survey of Canada, Open File 6108, scale 1:50 000. https://doi.org/10.4095/247496

Kiss, F. and Coyle, M., 2009d. First vertical derivative of the magnetic field, McQuesten aeromagnetic survey, NTS 115-I/15, Yukon / Dérivée première verticale du champ magnétique, levé aéromagnétique McQuesten, SNRC 115-I/15, Yukon; Geological Survey of Canada, Open File 6109, scale 1:50 000. https://doi.org/10.4095/247497

Kiss, F. and Coyle, M., 2009e. Residual total magnetic field, McQuesten aeromagnetic survey, NTS 115 J/16 and part of 115 J/15, Yukon / Composante résiduelle du champ magnétique total, levé aéromagnétique McQuesten, SNRC 115 J/16 et partie de 115 J/15, Yukon; Geological Survey of Canada, Open File 6110, scale 1:50 000. https://doi.org/10.4095/247498

Kiss, F. and Coyle, M., 2009f. First vertical derivative of the magnetic field, McQuesten aeromagnetic survey, NTS 115 J/16 and part of 115 J/15, Yukon / Dérivée première verticale du champ magnétique, levé aéromagnétique McQuesten, SNRC 115 J/16 et partie de 115 J/15, Yukon; Geological Survey of Canada, Open File 6111, scale 1:50 000. https://doi.org/10.4095/247499

Kiss, F. and Coyle, M., 2009g. Residual total magnetic field, McQuesten aeromagnetic survey, NTS 115-O/1 and 115-O/2, Yukon / Composante résiduelle du champ magnétique total, levé aéromagnétique McQuesten, SNRC 115-O/1 et 115-O/2, Yukon; Geological Survey of Canada, Open File 6112, scale 1:50 000. https://doi.org/10.4095/247500

Kiss, F. and Coyle, M., 2009h. Residual total magnetic field, Northern Stevenson Ridge aeromagnetic survey, NTS 115 J/9 and 115 J/10, Yukon / Composante résiduelle du champ magnétique total, levé aéromagnétique de la partie nord de Stevenson Ridge, SNRC 115 J/9 et 115 J/10, Yukon; Geological Survey of Canada, Open File 6254, scale 1:50 000. https://doi.org/10.4095/248160

Kiss, F. and Coyle, M., 2009i. First vertical derivative of the magnetic field, Northern Stevenson Ridge aeromagnetic survey, NTS 115 J/9 and 115 J/10, Yukon / Dérivée première verticale du champ magnétique, levé aéromagnétique de la partie nord de Stevenson Ridge, SNRC 115 J/9 et 115 J/10, Yukon; Geological Survey of Canada, Open File 6255, scale 1:50 000. https://doi.org/10.4095/248161

Kiss, F. and Coyle, M., 2009j. Residual total magnetic field, Northern Stevenson Ridge aeromagnetic survey, NTS 115 J/11 and 115 J/12, Yukon / Composante résiduelle du champ magnétique total, levé aéromagnétique de la partie nord de Stevenson Ridge, SNRC 115 J/11 et 115 J/12, Yukon; Geological Survey of Canada, Open File 6256, scale 1:50 000. https://doi.org/10.4095/248162

Kiss, F. and Coyle, M., 2009k. First vertical derivative of the magnetic field, Northern Stevenson Ridge aeromagnetic survey, NTS 115 J/11 and 115 J/12, Yukon / Dérivée première verticale du champ magnétique, levé aéromagnétique de la partie nord de Stevenson Ridge, SNRC 115 J/11 et 115 J/12, Yukon; Geological Survey of Canada, Open File 6257, scale 1:50 000. https://doi.org/10.4095/248163

Kiss, F. and Coyle, M., 2009l. Residual total magnetic field, Northern Stevenson Ridge aeromagnetic survey, NTS 115 J/13 and 115 J/14, Yukon / Composante résiduelle du champ magnétique total, levé aéromagnétique de la partie nord de Stevenson Ridge, SNRC 115 J/13 et 115 J/14, Yukon; Geological Survey of Canada, Open File 6258, scale 1:50 000. https://doi.org/10.4095/248164

Kiss, F. and Coyle, M., 2009m. First vertical derivative of the magnetic field, Northern Stevenson Ridge aeromagnetic survey, NTS 115 J/13 and 115 J/14, Yukon / Dérivée première verticale du champ magnétique, levé aéromagnétique de la partie nord de Stevenson Ridge, SNRC 115 J/13 et 115 J/14, Yukon; Geological Survey of Canada, Open File 6259, scale 1:50 000. https://doi.org/10.4095/248165

Kiss, F. and Coyle, M., 2011a. Residual total magnetic field, aeromagnetic survey of the Nisling River area, parts of NTS 115 G/8, 9 and H/5, 12, Yukon / Composante résiduelle du champ magnétique total, levé aéromagnétique de la région de la rivière Nisling, SNRC parties de 115 G/8, 9 et H/5, 12, Yukon; Geological Survey of Canada, Open File 6891, scale 1:50 000. https://doi.org/10.4095/288926

Kiss, F. and Coyle, M., 2011b. First vertical derivative of the magnetic field, aeromagnetic survey of the Nisling River area, parts of NTS 115 G/8, 9 and H/5, 12, Yukon / Dérivée première verticale du champ magnétique, levé aéromagnétique de la région de la rivière Nisling, SNRC parties de 115 G/8, 9 et H/5, 12, Yukon; Geological Survey of Canada, Open File 6892, scale 1:50 000. https://doi.org/10.4095/288930

Kiss, F. and Coyle, M., 2011c. Residual total magnetic field, aeromagnetic survey of the Nisling River area, parts of NTS 115 G/10, 11, Yukon / Composante résiduelle du champ magnétique total, levé aéromagnétique de la région de la rivière Nisling, SNRC parties de 115 G/10, 11, Yukon; Geological Survey of Canada, Open File 6893, scale 1:50 000. https://doi.org/10.4095/288932

Kiss, F. and Coyle, M., 2011d. First vertical derivative of the magnetic field, aeromagnetic survey of the Nisling River area, parts of NTS 115 G/10, 11, Yukon / Dérivée première verticale du champ magnétique, levé aéromagnétique de la région de la rivière Nisling, SNRC parties de 115 G/10, 11, Yukon; Geological Survey of Canada, Open File 6894, scale 1:50 000. https://doi.org/10.4095/288933

Kiss, F. and Coyle, M., 2011e. Residual total magnetic field, aeromagnetic survey of the Nisling River area, part of NTS 115 G/13, Yukon / Composante résiduelle du champ magnétique total, levé aéromagnétique de la région de la rivière Nisling, SNRC partie de 115 G/13, Yukon; Geological Survey of Canada, Open File 6895, scale 1:50 000. https://doi.org/10.4095/288934

Kiss, F. and Coyle, M., 2011f. First vertical derivative of the magnetic field, aeromagnetic survey of the Nisling River area, part of NTS 115 G/13, Yukon / Dérivée première verticale du champ magnétique, levé aéromagnétique de la région de la rivière Nisling, SNRC partie de 115 G/13, Yukon; Geological Survey of Canada, Open File 6896, scale 1:50 000. https://doi.org/10.4095/288935

Kiss, F. and Coyle, M., 2011g. Residual total magnetic field, aeromagnetic survey of the Nisling River area, NTS 115 G/15 and part of 115 G/14, Yukon / Composante résiduelle du champ magnétique total, levé aéromagnétique de la région de la rivière Nisling, SNRC 115 G/15 et partie de 115 G/14, Yukon; Geological Survey of Canada, Open File 6897, scale 1:50 000. https://doi.org/10.4095/288936

Kiss, F. and Coyle, M., 2011h. First vertical derivative of the magnetic field, aeromagnetic survey of the Nisling River area, parts of NTS 115 G/15 and part of 115 G/14, Yukon / Dérivée première verticale du champ magnétique, levé aéromagnétique de la région de la rivière Nisling, SNRC 115 G/15 et partie de 115 G/14, Yukon; Geological Survey of Canada, Open File 6898, scale 1:50 000. https://doi.org/10.4095/288937

Kiss, F. and Coyle, M., 2014a. Residual total magnetic field, aeromagnetic survey of the Dawson area, NTS 115-N/15 and parts of 115-N/7, 115-N/9, 115-N/10, 115-N/16 and 115-O/13, Yukon; Geological Survey of Canada, Open File 7634, scale 1:100 000. https://doi.org/10.4095/295105

Kiss, F. and Coyle, M., 2014b. First vertical derivative of the magnetic field, aeromagnetic survey of the Dawson area, NTS 115-N/15 and parts of 115-N/7, 115-N/9, 115-N/10, 115-N/16 and 115-O/13, Yukon; Geological Survey of Canada, Open File 7635, scale 1:100 000. https://doi.org/10.4095/295106

Kiss, F. and Coyle, M., 2014c. Residual total magnetic field, aeromagnetic survey of the Dawson area, NTS parts of 115-O/14, 115-O/15, 115-O/16, 116-B/1, 116-B/2, 116-B/3, 116-B/6 and 116-B/7, Yukon; Geological Survey of Canada, Open File 7636, scale 1:100 000. https://doi.org/10.4095/295107

Kiss, F. and Coyle, M., 2014d. First vertical derivative of the magnetic field, aeromagnetic survey of the Dawson area, NTS parts of 115-O/14, 115-O/15, 115-O/16, 116-B/1, 116-B/2, 116-B/3, 116-B/6 and 116-B/7, Yukon; Geological Survey of Canada, Open File 7637, scale 1:100 000. https://doi.org/10.4095/295108

Kiss, F. and Coyle, M., 2014e. Residual total magnetic field, aeromagnetic survey of the Dawson area, NTS 116-B/4, 116-B/5, 116-C/1, 116-C/2, 116-C/7 and 116-C/8, Yukon; Geological Survey of Canada, Open File 7638, scale 1:100 000. https://doi.org/10.4095/295109

Kiss, F. and Coyle, M., 2014f. First vertical derivative of the magnetic field, aeromagnetic survey of the Dawson area, NTS 116-B/4, 116-B/5, 116-C/1, 116-C/2, 116-C/7 and 116-C/8, Yukon; Geological Survey of Canada, Open File 7639, scale 1:100 000. https://doi.org/10.4095/295110

Kiss, F. and Coyle, M., 2014g. Residual total magnetic field, aeromagnetic survey of the Dawson area, NTS 116-C/9, 116-C/10 and parts of 116-B/11, 116-B/12, 116-C/15 and 116-C/16, Yukon; Geological Survey of Canada, Open File 7640, scale 1:100 000. https://doi.org/10.4095/295111

Kiss, F. and Coyle, M., 2014h. First vertical derivative of the magnetic field, aeromagnetic survey of the Dawson area, NTS 116-C/9, 116-C/10 and parts of 116-B/11, 116-B/12, 116-C/15 and 116-C/16, Yukon; Geological Survey of Canada, Open File 7641, scale 1:100 000. https://doi.org/10.4095/295112

Miles, W., Saltus, R., Hayward, N., and Oneschuk, D., 2017. Alaska and Yukon magnetic compilation, residual total magnetic field. Geological Survey of Canada, Open File 7862, scale 1:1 120 000. https://doi.org/10.4095/301695

Moynihan, D., 2016a. Bedrock geology of the upper Hyland River area, NTS 105H/8, 9, 10, 15, 16 and 105I/2, southeast Yukon; Yukon Geological Survey, Open File 2016-36, scale 1:50 000.

Moynihan, D., 2016b. Stratigraphy and structural geology of the upper Hyland River area (parts of 105H/8, 105H/9), southeast Yukon; *in* Yukon Exploration and Geology 2015, (ed.) K.E. MacFarlane and M.G. Nordling; Yukon Geological Survey, p. 187–206.

Moynihan, D., 2017. Progress report on geological mapping in the upper Hyland River region of southeastern Yukon (parts of NTS 105H/08,09,10,15,16 and 105I/02); *in* Yukon Exploration and Geology 2016, (ed.) K.E. MacFarlane and L.H. Weston, Yukon Geological Survey, p. 163–180.

Oneschuk, D.; Miles, W.; Saltus, R.; Hayward, N., 2019. Alaska and Yukon magnetic compilation, residual total magnetic field; Geological Survey of Canada, Open File 7862, (version 2.0), scale 1:1 120 000. https://doi.org/10.4095/313537

Reiners, P.W. and Brandon, M.T., 2006. Using thermochronology to understand orogenic erosion; Annual Review of Earth and Planetary Sciences, v. 34, p. 419–466. https://doi.org/10.1146/annurev.earth.34.031405.125202

Ryan, J.J., Colpron, M., and Hayward, N., 2010. Geology, southwestern McQuesten and parts of northern Carmacks, Yukon. Geological Survey of Canada, Canadian Geoscience Map 7, scale 1:125 000. https://doi.org/10.4095/287154

Ryan, J.J., Zagorevski, A., Williams, S.P., Roots, C., Ciolkiewicz, W., Hayward, N., and Chapman, J.B., 2013a. Geology, Stevenson Ridge (northeast part), Yukon; Geological Survey of Canada, Canadian Geoscience Map 116, scale 1:100 000. https://doi.org/10.4095/292407

Ryan, J.J., Zagorevski, A., Williams, S.P., Roots, C., Ciolkiewicz, W., Hayward, N., and Chapman, J.B., 2013b. Geology, Stevenson Ridge (northwest part), Yukon; Geological Survey of Canada, Canadian Geoscience Map 117, scale 1:100 000. https://doi.org/10.4095/292408

Ryan, J.J., Westberg, E.E., Williams, S.P., and Chapman, J.B., 2016. Geology, Mount Nansen - Nisling River area, Yukon; Geological Survey of Canada, Canadian Geoscience Map 292, scale 1:100 000. https://doi.org/10.4095/298835

Ryan, J.J., Hayward, N., and Jackson, L.E., 2017. Landscape antiquity and Cenozoic drainage development of southern Yukon, through restoration modeling of the Tintina Fault; Canadian Journal of Earth Sciences, v. 54, p. 1085–1100. https://doi.org/10.1139/cjes-2017-0053

Ryan, J.J., Israel, S., Williams, S.P., Parsons, A.J., and Hayward, N., 2018. Bedrock geology, Klaza River area, Yukon; Geological Survey of Canada, Canadian Geoscience Map 376, scale 1:100 000. https://doi.org/10.4095/311301

van Staal, C.R., Zagorevski, A., McClelland, W.C., Escayola, M.P., Ryan, J.J., Parsons, A.J., and Proenza, J., 2018. Age and setting of Permian Slide Mountain terrane ophiolitic ultramafic-mafic complexes in the Yukon: implications for late Paleozoic-early Mesozoic tectonic models in the northern Canadian Cordillera; Tectonophysics, v. 744, p. 458–483. https://doi.org/10.1016/j.tecto.2018.07.008

Yukon Geological Survey, 2011. Bouguer gravity anomaly of the northern Aishihik Lake area, Yukon (parts of NTS 115H, I and G); Yukon Geological Survey, Open File 2011-27, scale 1:250 000.

Yukon Geological Survey, 2012. Bouguer gravity anomaly of the northern Aishihik Lake area, Yukon (parts of NTS 105E, L and 115H, I); Yukon Geological Survey, Open File 2012-30, scale 1:250 000.

Yukon Geological Survey, 2018. Update of the Yukon bedrock geology map; Yukon Geological Survey. <http://www.geology.gov.yk.ca/update_yukon_bedrock_geology_map.html> [accessed August 20, 2018]